

Using an oceanographic model to investigate the mystery of the missing puerulus

Jessica Kolbusz¹, Tim Langlois², Charitha Pattiaratchi¹, Simon de Lestang³

¹ Oceans Graduate School and the UWA Oceans Institute, The University of Western Australia, Crawley, WA 6009, Australia

² School of Biological Sciences and the UWA Oceans Institute, The University of Western Australia, Crawley, WA, Australia

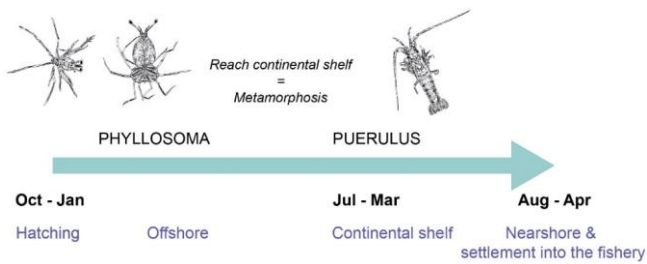
³ Western Australian Fisheries and Marine Research Laboratories, Department of Primary Industries and Regional Development, Government of Western Australia, North Beach, WA, Australia

Correspondence to: Jessica Kolbusz (jessica.kolbusz@research.uwa.edu.au)

Abstract. Dynamics of ocean boundary currents and associated shelf processes can influence onshore/offshore ~~transport-of~~ ~~water~~ ~~water transport~~, critically impacting marine organisms that release long-lived pelagic larvae into the water column. The western rock lobster, *Panulirus cygnus*, endemic to Western Australia, is the basis of Australia's most valuable wild-caught commercial fishery. After hatching, western rock lobster larvae (phyllosoma) spend up to 11 months in offshore waters before ocean currents and their ability to swim; ~~transports~~ them back to the coast. The abundance of western rock lobster ~~post-larvae~~ (puerulus) (~~settlement phase post-phyllsoma~~) ~~has historically been observed to be positively correlated with the strength of the Leeuwin Current, and provides a puerulus index-an index of puerulus numbers~~ is used by fisheries managers as a predictor of ~~subsequent~~ lobster abundance 3-4 years later. ~~This index has historically been positively correlated with the strength of the Leeuwin Current.~~ In 2008 and 2009, the Leeuwin Current was strong, yet a settlement failure occurred throughout the fishery, prompting management changes and a rethinking of environmental factors associated with their settlement. Thus, understanding factors that may have been responsible for the settlement failure ~~is-are important-essential~~ for fisheries management. Oceanographic parameters likely to influence puerulus settlement were derived for a ~~17-year period~~ ~~17 years~~ to investigate correlations. Analysis indicated that puerulus settlement at adjacent monitoring sites have similar oceanographic forcing with kinetic energy in the offshore and the strength of the Leeuwin Current being key factors. Settlement failure years were synonymous with 'hiatus' conditions in the south-east Indian Ocean; and periods of sustained cooler water present offshore. ~~Post-Post-2009~~, there has been an unusual but consistent increase in the Leeuwin Current during the early summer months with a matching decrease in the Capes Current, ~~that-which~~ may explain an observed settlement timing mismatch compared to historical data. Our study has revealed that a culmination of these conditions likely led to the recruitment failure and subsequent changes in puerulus settlement patterns.

1 Introduction

30 Fisheries management of the western rock lobster (*Panulirus cygnus*), Australia's most valuable wild-caught single-species fishery (de Lestang et al., 2018), ~~utilises~~ utilizes an index of *P. cygnus* post-larvae (puerulus) settlement as one of its main-leading stock diagnostics. Over the past four decades, this index has been used to predict catches 3 to 4 years in advance (Phillips, 1986; Caputi and Brown, 1993; de Lestang et al., 2015), ~~while and puerulus settlement was historically observed to~~ being positively correlated with the strength of the Leeuwin Current (Pearce and Phillips, 1988; Lenanton et al., 1991).
35 ~~During the 2008 and 2009 settlement seasons (May—April) there was an unexpected~~ There was an unexpected decline in puerulus settlement numbers during the 2008 and 2009 settlement seasons (May - April). ~~given the strong Leeuwin Current over those years, settlement failure.~~ In response to this, the Department of Primary Industries and Regional Development, Western Australia (DPIRD, WA) fisheries managers made ~~large~~ significant reductions to landings ~~and~~. In addition, they restructured the management system from input to output controls (Caputi et al., 2021). Puerulus settlement has subsequently
40 recovered, but despite extensive research regarding overfishing or possible biological and oceanographic conditions causing the change (de Lestang et al., 2015; Säwström et al., 2014), no clear ~~apparent~~ discernible factor(s) explaining the puerulus settlement failure ~~decline~~ have been identified to date. ~~Recent~~ Other research has shown that, since the recovery in puerulus numbers, there has been a latitudinal and timing shift in puerulus settlement compared to historical data (Kolbusz et al., 2021). ~~(Kolbusz et al., 2021).~~ The majority of the reduction in ~~has~~ occurred in the first half of the puerulus settlement season (May
45 - October; Kolbusz et al., 2021). Additionally, in the southern sites, there has been a significant reduction over the whole season. In contrast, those in the north have maintained levels of puerulus settlement during the second half of the season (Kolbusz et al., 2021).



50 Figure 1 Early life-cycle schematic of *P. cygnus*. Below the arrow indicates each stage's approximate timing (black) and location (blue). Above the arrow displays their growth, image credit Alice Ford.

Between November and February, berried western rock lobster females release their larvae (phyllosoma) throughout the study region (Figure 1, Figure 2a). They are then transported offshore by the prevailing currents into the open ocean, where they transform through a series of temperature-dependent moults (Figure 1). They undergo their final metamorphosis into the actively swimming nektonic puerulus after approximately eight months (Figure 1). The onshore movement of puerulus across

55 the continental shelf peaks between September and February (Phillips, 1981; de Lestang et al., 2018). Therefore, circulation
patterns of the south-east Indian Ocean influence spatially varied cross-shelf transport of the puerulus (Caputi, 2008; Feng et
al., 2011). After a maximum of approximately 30 days, they reach shallow areas of reef and seagrass habitats as early juveniles
(Feng et al., 2011).

60 In the late 1960s, puerulus collectors resembling artificial seaweed were developed and deployed at several shallow-
water sites within the fishery (Phillips 1981). Puerulus are currently counted at eight sites spanning the latitude of the fishery,
with the centrally-located Dongara collectors (Figure 2a) now providing over 50 years of *in-situ* data (Kolbusz et al., 2021).
The puerulus settlement index (puerulus index, PI) is derived from this data, with the majority of puerulus settlement occurring
between August and January(de Lestang et al., 2012). Therefore the puerulus settlement season occurs between May to April.

65 Research on the interaction between the physical environment and PI began in the 1980s with a strong positive
relationship found between the strength of the Leeuwin Current (LC), with Fremantle Mean Sea Level (FMSL) as a proxy
(Pearce and Phillips, 1988; Lenanton et al., 1991). Consequently, La Niña phases were also found to coincide with an above-
average PI, thought to be due to a strengthened LC during these phases, with the Southern Oscillation Index (SOI) as an
indicator of El Niño Southern Oscillation phases (Clarke and Li, 2004; Caputi et al., 2001; Pearce and Phillips, 1988). These
relationships were identified through long-term correlations between the PI, FMSL, and SOI (Figure 3). Since 1988, studies
70 have also demonstrated that the inter-annual variation in PI was influenced by the sea surface temperature (SST) and westerly
(onshore) winds (Caputi and Brown, 1993; Caputi, 2008; Caputi et al., 2010). Caputi et al. (2001) defined a significant area
overlapping with the spatial extent of the LC, where SST (27°–34°S, 105°–117°E) in February-April had a positive relationship
with the PI of the subsequent season. The bottom temperature during the spawning season has also been identified as a cue for
hatching and therefore has a possible influence on the puerulus settlement season to follow (Chittleborough, 1975; de Lestang
75 et al., 2015).

This study aims to better understand why this recruitment failure occurred in 2008 and 2009, and why there has been
a change in the timing and latitude before and after these years, particularly in relation to oceanographic processes. Since
2009, the majority of the reduction in the settlement of puerulus has occurred in the first half of the settlement season (May –
October; Kolbusz et al., 2021). Additionally, in the southern sites, there has been a significant reduction over the whole season,
80 whereas those in the north have maintained levels of settlement during the second half of the season. Prior to current study,
research on the 2008/09 decline had included an examination of overfishing of the spawning stock (de Lestang et al., 2015)
and whether conditions of survival were no longer met in the early pelagic life stages (Sävström et al., 2014). Given the recent
research revealing a mismatch in the timing of settlement, compared to historical norms (Kolbusz et al., 2021) the current
study set out to further investigate the environmental factors that may have led to the changes in puerulus settlement.

85

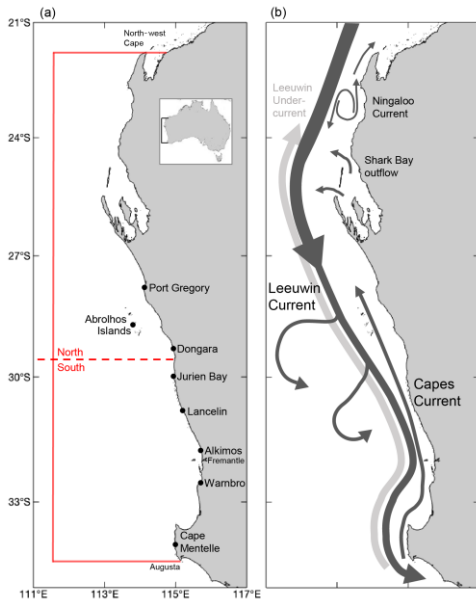


Figure 2 (a) Locations of puerulus survey sites included within this study and other locations of note. The north and south refer to the midpoint used in this analysis. In particular for kinetic and eddy kinetic energy calculation. Red boundary is the extent of environmental variables. Inset shows location of the coastline in Australia (b) Schematic of the major currents systems thought to influence early-stage *P. cygnus* larvae movement. Relative arrow size and location show characteristic currents. Eddies generated by the LC flow down the continental shelf are also seen indicated.

Following the decline in the PI in 2008 and 2009 (Figure 3), the aforementioned relationships between the PI and oceanographic factors broke down (de Lestang et al., 2015; Caputi et al., 2014; Feng et al., 2011). Through one of the strongest La Niña phases on record, the PI still did not recover to the previously expect high values (2011) (Boening et al., 2012; Benthuisen et al., 2014). These changes have been generally attributed to increasing water temperatures during the spawning period, resulting in an earlier onset of spawning, and a decrease in the number of storms occurring near puerulus settlement (de Lestang et al., 2015). Since this decoupling of oceanographic parameters and PI, additional years of contrasting settlement have been recorded, thus providing a larger dataset to re-examine these relationships following the period of low settlement.

Between November and February, berried western rock lobster females release their larvae (phyllosoma) throughout the study region (Figure 1a), which they are then transported offshore by the prevailing ocean currents into the deeper open ocean, where they transform over nine larval stages through a series of temperature-dependent moults (Figure 2). Finally, at around eight months, they undergo their final metamorphosis into the actively swimming nektonic puerulus after approximately eight months (post larval stage) (Figure 2). The onshore transport movement of puerulus across the conand

movement across the continental shelf occurs peaks between mainly during August-September and February-January (late austral winter-summer) to settle in shallow areas of generally less than 5 metres depth (Phillips, 1981; de Lestang et al., 2018). Circulation patterns of the south-east Indian Ocean. Therefore, circulation patterns of the south-east Indian Ocean influence spatially varied cross-shelf transport of the puerulus (Caputi, 2008; Feng et al., 2011) likely influence spatially varied cross-shelf transport of the puerulus (Caputi, 2008; Feng et al., 2011b). After a maximum of 30 days, they reach shallow areas of reef and seagrass habitats as early juveniles.

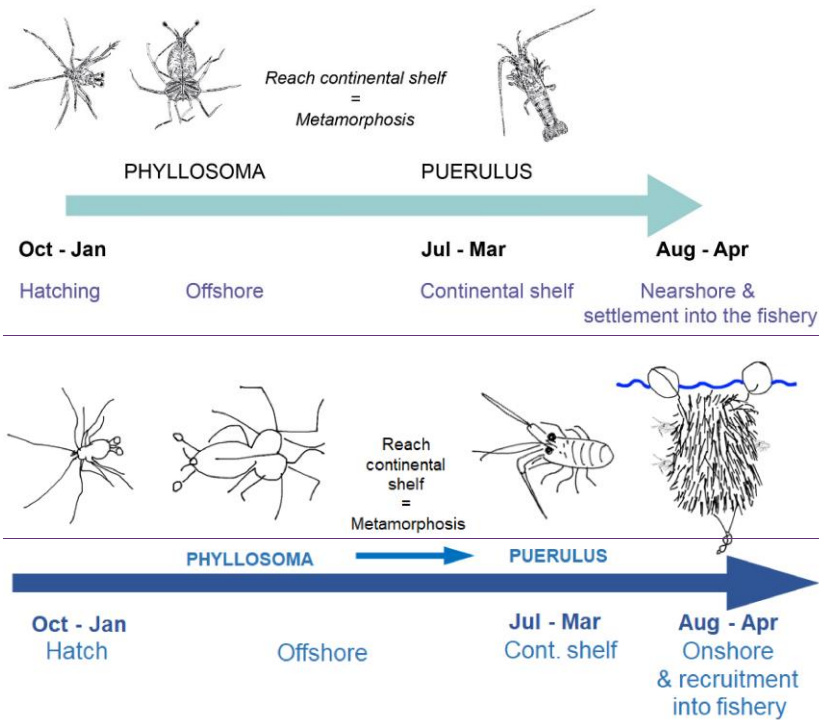


Figure 2 Early life cycle schematic of *P. cygnus*. Below the arrow indicates the approximate timing and location of each stage each stage's approximate timing (black) and location (blue). Above the arrow displays their growth, image credit Alice Ford and eventual recruitment into the fishery where they are collected.

In the late 1960's, puerulus collectors resembling artificial seaweed were developed and deployed at several shallow water sites within the fishery (Phillips 1981). Puerulus numbers are currently collected/ counted at eight sites spanning the latitude of the fishery, with the centrally located Dongara collectors (Figure 1) now providing over 50 years of *in situ* data (Kolbusz et al., 2021). The Since a majority of the settlement occurs between August and January, Therefore the settlement

Formatted: Not Highlight

Formatted: Not Highlight

~~season occurs between May to April.~~ The puerulus settlement index and very little occurs between April and May, the puerulus settlement index (puerulus index, PI) is derived from these ~~this data~~ (puerulus index, PI), with the majority of puerulus settlement occurring between August and January. ~~Therefore the puerulus settlement season occurs between May to April.~~ is standardised to a 12-month period spanning May to the following April and is the mean of the sum of puerulus counted at all sites during each full moon (i.e. approximately monthly).

Research on the interaction between the physical environment and PI began in the 1980s with a strong positive relationship found between the strength of the Leeuwin Current (LC), with Fremantle Mean Sea Level (FMSL) as a proxy (Pearce and Phillips, 1988; Lenanton et al., 1991). Consequently, La Niña phases were also found to coincide with an above-average PI, thought to be due to a strengthened LC during these phases, with the Southern Oscillation Index (SOI) as an indicator of El Niño Southern Oscillation phases (Clarke and Li, 2004; Caputi et al., 2001; Pearce and Phillips, 1988). These relationships were identified through long-term correlations between the PI_t and both FMSL_t and SOI (Figure 3). Since 1988, studies have also demonstrated ~~that~~ the inter-annual variation in PI was influenced by the sea surface temperature (SST) and westerly (onshore) winds (Caputi and Brown, 1993; Caputi, 2008; Caputi et al., 2010). Caputi et al. (2001) defined a significant area overlapping with the spatial extent of the LC, where SST (27°–34°S, 105°–117°E) in February–April had a positive relationship with the PI of the subsequent season. ~~Bottom~~ ~~The bottom~~ temperature during ~~the spawning season~~ has also been identified as a cue for spawning ~~hatching and therefore has a possible influence on the puerulus settlement season to follow~~ (Chittleborough, 1975; de Lestang et al., 2015). In addition, westerly winds, associated with storms in late winter to spring, have been related to an increased PI for the coming season (Caputi et al., 2010).

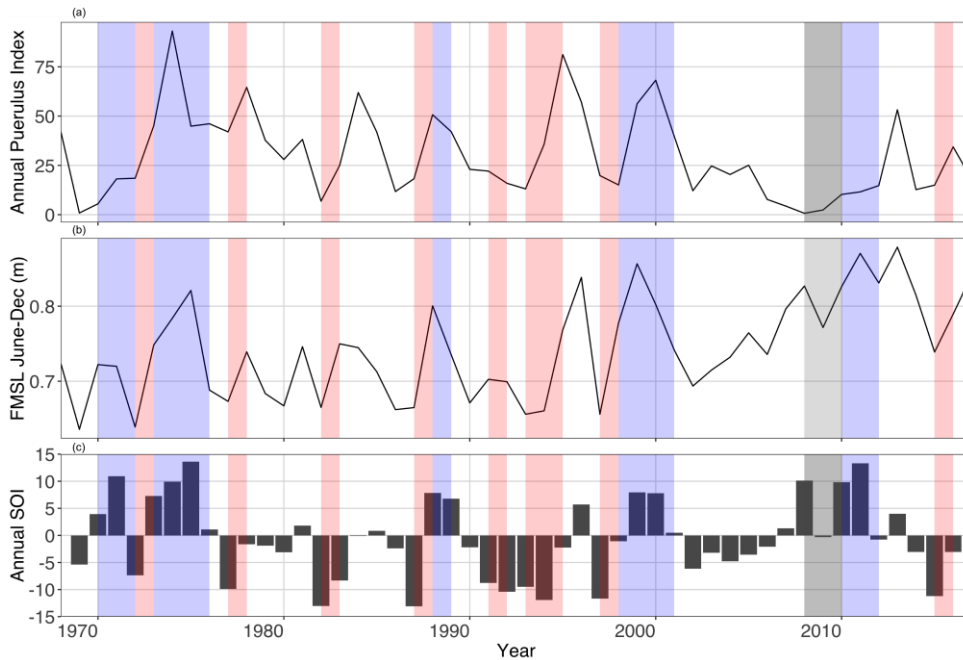


Figure 13 Time series of annual (a) fishery-wide Puerulus Index (PI) (May – April); (b) Fremantle Mean Sea Level (FMSL) over June to December (m); and, (c) Southern Oscillation Index (SOI) (May –April). Grey shaded seasons indicate the less than expected PI based on a priori relationships (Caputi et al. 2001). Blue and red shading indicates a La Niña and El Niño periods, respectively. Updated to 2018 and modified from Figure 5 in Caputi et al. 2001.

Over two consecutive years (2008 to 2009), an abnormally low PI occurred prompting management changes and a re-evaluation of environmental drivers of puerulus settlement (Figure 3) (Caputi et al., 2014a; de Lestang et al., 2015) (de Lestang et al. 2014; Caputi et al. 2014). In 2008, the settlement was expected to be above average due to the presence of warm offshore water temperatures in early 2007 and a high FMSL (Figure 3), but instead was a record low, which was then followed by the second lowest settlement in 2009. Below average PI was recorded for seven consecutive seasons (2006 – 2012) (de Lestang et al., 2015) and through one of the strongest La Niña phases on record (2011) (Boening et al., 2012). Following this the period of decline, previous relationships between PI and oceanographic factors have broken down and the correspondence between FMSL and SOI and puerulus settlement no longer exist (decline in the PI in 2008 and 2009 (Figure 3), the aforementioned previous relationships between the PI and oceanographic factors broke down (de Lestang et al., 2015; Caputi et al., 2014; Feng et al., 2011). Namely, the correspondence between FMSL and SOI and PI no longer exists (Figure 3) (de Lestang et al., 2015; Caputi et al., 2014; Feng et al., 2011). Through one of the strongest La Niña phases on record, the PI still

155 ~~did not recover to the previously expect high values (2011) (Boening et al., 2012; Benthuyesen et al., 2014) (de Lestang et al., 2015; Caputi et al., 2014a). These changes have been attributed to shifting oceanographic conditions relating to increasing water temperatures during the spawning period resulting in an earlier onset of spawning, and a decrease in the number of storms occurring near the time of puerulus settlement (de Lestang et al., 2015).~~

160 ~~Since 2009, the majority of the reduction in the settlement of puerulus has occurred in the first half of the settlement season (May–October; Kolbusz et al., 2021). Additionally, in the southern sites, there has been a significant reduction over the whole season, whereas those in the north have maintained levels of settlement during the second half of the season. Prior to current study, research on the 2008/09 decline had included an examination of overfishing of the spawning stock (de Lestang et al., 2015) and whether conditions of survival were no longer met in the early pelagic life stages (Sawström et al., 2014). Given the recent research revealing a mismatch in the timing of settlement, compared to historical norms (Kolbusz et al., 2021) the current study set out to further investigate the environmental factors that may have led to the changes in puerulus settlement.~~

165 ~~Since the apparent his decoupling of some oceanographic parameters and puerulus settlement PI, and the initial research into the anomaly, additional years of contrasting settlement have have been recorded, thus providing a larger dataset to re-examine these relationships following the period of low settlement.~~

170 ~~In addition, recent studies have shown changes in inter-annual ocean variability in both the southwest of Australia and along the whole coastline, with an increase in the number of storms occurring and shifting to later in the year (Wandres et al., 2017). Studying direct physical oceanographic parameters likely to influence phyllosoma on during their pelagic phase offshore and eventual coastal life cycle, provides an opportunity to investigate local variation in puerulus settlement. We can also better understand or whether long term trends and lagging effects are at play. For example, the causal factors of the correlation between LC strength and puerulus settlement index prior to before 2009 is are unknown, whether it was due to the warmer waters the LC brings, or higher eddy retention of larvae close to the coast and therefore better nutritional development of *P. cygnus* (Caputi et al., 2001; O'Rorke et al., 2015; Wang et al., 2015; Lenanton et al., 1991). On the shelf, the northward northward flowing Capes Current (CC) is additionally suspected to correspond with the offshore movement in the early larval stages (October–March) from the coast coast (Feng et al., 2011). (Feng et al., 2011);~~

180 ~~The recent availability of high resolution numerical oceanographic model output over an extended period (Wijeratne et al., 2018) eliminates the need to use proxies to represent oceanographic parameters likely to influence larvae transport. Alongside direct predicted values of the LC, CC and temperature we were able to calculate oceanographic parameters which have not been previously examined against puerulus settlement. This includes kinetic energy (KE), eddy kinetic energy (EKE) and cross-shelf transport. This study aims to understand the recruitment failure and subsequent shifts in settlement patterns, particularly regarding direct physical oceanographic parameters over the 9 to 11 months before settlement oceanographic processes. Previous research has highlighted that the causal factor of the correlation between the LC strength and PI before 2009 was unclear. Several suggestions have been made as to whether it was Whether it was due to the warmer waters the LC brings, high eddy retention of larvae close to the coast, or better nutritional development within eddies (Caputi et al., 2001; O'Rorke et al., 2015; Wang et al., 2015; Lenanton et al., 1991). Other parameters defining the oceanographic conditions in the~~

Field Code Changed

region, including the northward-flowing Capes Current (CC) (Figure 2b), cross-shelf flows and the Kinetic and Eddy Kinetic energy, have been previously suggested but not investigated (Hood et al., 2017; Koslow et al., 2008). The recent availability of high resolution 3D numerical oceanographic model output over an extended period (Wijeratne et al., 2018) eliminates the need to use proxies to represent oceanographic parameters likely to influence larvae transport processes. Therefore we were able to calculate directly predicated oceanographic parameters at various locations throughout the fishery to investigate alongside puerulus settlement. Alongside direct predicted values of the LC, CC and temperature we were able to calculate oceanographic parameters which have not been previously examined against puerulus settlement. Instead, we calculated directly predicted LC, CC, and temperature values. This included different latitudinal values for the current strengths. Predictor variables which have not been used previously are kinetic energy (KE), eddy kinetic energy (EKE) and cross shelf transport. Spatially they provided an overall value for are d oceanographic parameters that have not been previously examined against puerulus settlement alongside. This We also included kinetic energy (KE), eddy kinetic energy (EKE) and cross shelf transport. Using these The aim of this paper is to use numerical model outputs and satellite data (sea surface temperature, SST), to we identify fy physical oceanographic variables, and biological information on estimates of western rock lobster spawning biomass western rock lobster spawning biomass, to investigate observed variations in PI over the past two decades. oceanographic structures and physical propertie

Field Code Changed

2 Study region

Water circulation off the west coast of Australia is driven by the Leeuwin Current (LC) System that incorporates the Leeuwin Current, the Leeuwin Undercurrent, and summer wind-driven currents, the Capes (CC) and Ningaloo (NC) currents, on the continental shelf (Figure 1b2b) (Woo and Pattiaratchi, 2008; Pattiaratchi and Woo, 2009). The LC is generated through a meridional pressure gradient resulting from the difference between lower density water off northwest Australia and the denser water of the Southern Ocean (Hamon, 1965; Pattiaratchi and Buchan, 1991; Pearce and Phillips, 1988). The mean southward volume transport of the LC peaks around 32.8° S, through input from due to South Indian Counter Current input (Wijeratne et al., 2018). Near 27–28° S statistical analysis has shown that there is a break-point in the LC, suggesting responses from the current's forcing along the coastline may differ on either side of this latitude (Chittleborough, 1976; Berthot et al., 2007). The El Niño Southern Oscillation (ENSO) cycle causes the pressure gradient to decrease/increase during an El Niño/La Niña episode, resulting in a weaker/stronger LC and cooler/warmer sea surface temperature SST (Pattiaratchi and Buchan, 1991; Feng et al., 2003; Wijeratne et al., 2018). This is supported with by strong correlations found between the Southern Oscillation Index (SOI as an indicator of ENSO phases) and LC transport at 34° S with a 6-month lag (Schiller et al., 2008). Surface current variability on the continental shelf within the study region is predominantly wind driven (Smith et al., 1991; Pattiaratchi et al., 1997). The LC is stronger during austral winter (May – July) and weaker during the austral summer

Field Code Changed

Field Code Changed

Field Code Changed

Field Code Changed

Field Code Changed

Field Code Changed

Field Code Changed

(November- March) due to variations in the equatorial wind stress and the Australasian monsoon season (January – March) (Pattiaratchi and Siji, 2020; Pattiaratchi and Woo, 2009; Smith et al., 1991; Wijeratne et al., 2018) ~~(Smith et al., 1991; Pattiaratchi and Woo, 2009; Wijeratne et al., 2018; Pattiaratchi et al., 2020)~~. A weaker secondary peak in the LC also occurs over December/January (Wijeratne et al., 2018). During the summer months, southerly wind stresses overcome the alongshore pressure gradient, moving upper layers offshore and favouring upwelling onto the continental shelf (Pearce and Pattiaratchi, 1999). ~~Surface current variability on the continental shelf within the study region is predominantly wind driven (Smith et al., 1991; Pattiaratchi et al., 1997)~~. The CC can be identified through cooler waters, ~~inshore of the LC and usually inshore of the 50-m contour, initiated around~~ $\sim 34^\circ$ S with the cooler water extending to 27° S- ~~inshore of the LC~~ (Figure 42b) (Gersbach et al., 1999). The LC migrates offshore and is weaker over these ~~predominantly~~ sea-breeze dominated summer months, whereas, during ~~autumn~~ winter, it floods the shelf and dominates the distribution of water masses (Cresswell et al., 1989; Pattiaratchi et al., 1997; Woo and Pattiaratchi, 2008).

Mesoscale eddies have been identified in the LC system for more than 30 years (Andrews, 1977; Pearce and Griffiths, 1991; Cosoli et al., 2020). The LC, and its associated flows, become unstable with the ~~large significant~~ variations in topography over the latitudinal extent of the current, generating eddies, meanders and offshoots (Batteen et al., 2007). ~~Therefore, As the LC strength increases, its eddies and meanders also increase~~ become more unstable, causing kinetic energy to increase (Feng et al., 2005; Pattiaratchi and Woo, 2009). The Abrolhos Islands at 28.8° S and the narrowing of the continental shelf slope south of Dongara and the Perth Canyon are major topographic features for the preferential generation of these eddies (Figure 42b) (Feng et al., 2005; Meuleners et al., 2008; Rennie et al., 2007; Huang and Feng, 2015; Cosoli et al., 2020). ~~Eddies in LC are mainly generated between 28° S and 33° S (Rennie et al., 2007; Fang and Morrow, 2003; Cosoli et al., 2020). As the LC strength increases, its eddies and meanders also increase, causing kinetic energy to increase (Feng et al., 2005; Pattiaratchi and Woo, 2009)~~. These mesoscale eddies have a mean radius of ~ 100 km and generally keep their original formation shape, lasting approximately ~~eight~~ 8 months (Fang and Morrow, 2003; Cosoli et al., 2020). ~~An increasing strength of the LC is replicated through increases in meanders and eddies down the coast, causing increases/decreases in austral winter/summer and increases/decreases during La Niña/El Niño phases (Feng et al., 2005; Pattiaratchi and Woo, 2009)~~.

3 Methods

3.1 Puerulus settlement data

Puerulus settlement is surveyed year-round, currently at eight sites across the fishery (between $34 - 27^\circ$ S) using artificial seagrass-like collectors (Figure 42a). Sampling is conducted as close as possible to the full moon, but may occur five days on either side. ~~Therefore, Puerulus puerulus~~ are likely to have settled on the previous new moon period, giving approximately monthly data (de Lestang et al., 2012). ~~The fishery wide standardized puerulus index, PI, is calculated based on the seasonal (May – April) mean puerulus settlement numbers from all 8 sites, then summed to obtain an annual index (Kolbusz et al., 2021)~~. The monthly puerulus settlement at each site is calculated as the average number of puerulus per

Field Code Changed

Field Code Changed

Field Code Changed

Field Code Changed

Field Code Changed

Field Code Changed

Field Code Changed

Field Code Changed

Field Code Changed

Field Code Changed

Field Code Changed

Field Code Changed

Field Code Changed

collector. For this study, we used the puerulus settlement data from ~~2000~~2001/02+ season to 2016/17 at each of the eight sites (Figure 4-2), aligned with ~~high-high~~-resolution oceanographic data ~~hereafter detailed (see below)~~ and estimates of western rock lobster spawning biomass. ~~Puerulus settlement data for each site was split into~~ Each site was treated separately, with analysis ~~between seasons being split into~~ “Early” (May – October) and “Late” (November – April) ~~portions, settlement~~ as described by Kolbusz et al. (2021).

3.2 Oceanographic data

~~To explore the variation in puerulus settlement, alongside the prevailing oceanographic conditions, a single value for the respective early or late puerulus portion of the season was determined. The variables were data was brought together simplified to be comparable to either the early or late puerulus settlement. Where relevant, the oceanographic variable was the same for both portions.~~

3.2.1 Numerical model outputs

The Regional Ocean Modelling System (ROMS) has been used in hindcast mode (past-time) for the whole of Australia (ozROMS) to resolve subsurface and surface currents and the associated volume transports (Wijeratne et al., 2018). This is a fully three-dimensional circulation model, resolving processes along the continental shelf, ~~which includes including~~ tides, setting it apart from other ocean models for the same region. The grid was set at a horizontal spacing of 3 km to allow for topographic detail, providing predicted water movement. ~~ozROMS-OzROMS~~ model output is available for the period 2000-2017 ~~for zonal (eastward) and meridional (northward) velocities, as well as temperature. Details and validation of the model are described by Wijeratne et al. (2018) including validation.~~ Examination of this predicted data set allows for the strength of the Leeuwin Current (LC), Capes Current (CC), and meridional and zonal cross-shore transport to be determined, as well as estimates of kinetic (KE) and eddy kinetic energy (EKE) ~~calculations~~ (Pattiaratchi and Siji, 2020). Their fluctuation is indicative of the conditions off the west coast of Australia.

Monthly surface KE and EKE was calculated from ozROMS to ~~characterise~~ characterize the variability in the currents. A monthly time series was estimated following Eq. (1) for KE and Eq. (2) for EKE:

$$KE = \sqrt{\frac{u^2 + v^2}{2}}, \quad (1)$$

$$EKE = \sqrt{\frac{u'^2 + v'^2}{2}}, \quad (2)$$

where u and v are the monthly mean meridional and zonal velocities, respectively (Caballero et al., 2008), and u' and v' are the monthly averages with the climatological means subtracted to remove seasonality (Luo et al., 2011). The months that phyllosoma are offshore, depending on when they have hatched, can be between October (year – 1) to March (year + 1) (Figure

Formatted: Border: Top: (No border), Bottom: (No border), Left: (No border), Right: (No border), Between : (No border)

280 2). Therefore, the calendar year from January to December was used to obtain an average for the offshore conditions spanning
the possible time frame offshore. Due to different mean oceanographic conditions, we considered a north and south offshore
box (Figure 1a) that covered Monthly KE and EKE values were then averaged to derive an annual mean value to align with
the average timing of phyllosoma being offshore (Jan to December, Figure 2). This was divided into a north and a south
offshore box of the approximate extent of where phyllosoma are transported and difference in observed settlement (Feng et
285 al., 2010; Berthot et al., 2007; Feng et al., 2011), (Figure 1, Kolbusz et al. 2021). For our analysis, we have not defined the
directionality and size of eddies. Still, it is an important consideration pertinent to larvae energy stores that would require
further modelling outside the scope of the current study (Cetina-Heredia et al., 2019b).

The monthly transport estimates of LC and CC (in Sverdrups, $Sv = 10^6 m^3 s^{-1}$) were derived using the ozROMS
hindcast dataset (Wijeratne et al., 2018). The transport for each current was defined as follows: (1) CC: as northward volume
290 transport of water across latitudes 27°S, 30°S and 34°S in water depths less than 100 m; and, (2) LC: as southward volume
transport of water across latitudes 27°S, 30°S and 34°S but in water depths greater than 100 m but limited to upper 300 m of
the water column (Table A1, Appendix A). For the LC austral winter strength, the transport over June, July and August was
averaged, and for summer, December, January and February was were averaged. The LC summer period corresponds to
recently hatched larvae leaving the continental shelf and puerulus returning in the “Late” portion of the season (Figure 2). The
305 LC winter period corresponds to when puerulus are returning to the shelf. The CC strength was divided into early (September,
October and November) and late (December, January, February and March) and corresponded to the time when recently
hatched larvae were leaving the continental shelf and puerulus returning in the “Early” and “Late” portions of the season
respectively (Figure 2).

Cross-shelf transport (in Sv) was calculated for each monthly time step between the depth contours (200 – 50 m) over
300 2 degree latitudinal bins (26 - 28° S, 28 - 30° S, 30 - 32° S and 32 - 34° S) (Table A1, Appendix 1). These latitudinal bins were
chosen closest to account for differences in topography and cross-shelf flow differences across the survey sites. Monthly
averages for each latitudinal bin indicated that the variability in transport is highest over April to September. These
months Cross-shelf transport at that time corresponds to the eastward “on” movement of puerulus. Recently hatched larvae
cross the shelf (westward, “off”) to the open ocean between September and March each season to align with the months that
305 phyllosomas are crossing the shelf (Figure 2). These two sets of months were averaged to get two values of cross-shelf
transport (westward as phyllosoma “off” and eastward as larvae “on”) for each season (Figure 2).

Temperatures in the model layer immediately above the seabed (“bottom temperature”) over the spawning depths (40
– 80 m) were retrieved from ozROMS due to the absence of in-situ data (de Lestang et al. 2015). The predicted data-values
were were averaged over a northern and southern subset (Figure 1a) of the data for the whole spawning season (September
310 September - March). Due to the ozROMS hindcast starting in 2000, values were only available from the 2001 season, since
the spawning season is the calendar year prior to settlement. Despite de Lestang et al. 2015 using monthly values, we
found only a small amount of variation between the months and therefore used a single bottom temperature value for the whole
season to represent a season. The temperature in the top 100 m of the water column, east of 108°E, as a mean annual value from

ozROMS was also included. This accounts for assumed phyllosoma distribution in south-east Indian Ocean (east of 108°E) as
315 mean annual value from ozROMS was also included. This accounts for temperature variation over the migrating depths
phyllosoma occupy over their pelagic-early pelagic life-cycle (Griffin et al. 2001; Feng et al. 2011).

3.2.2 Satellite-derived sea surface temperature (SST) and altimetry

Satellite-derived SST data for the study region were obtained from the Integrated Marine Observing System (IMOS)
Australian Ocean Data Network (AODN) portal (portal.aodn.org.au). The climatology data, centred on the base period 1993
320 – 2020, SST Atlas of Australian Regional Seas (SSTAARS) (Wijffels et al., 2018) were used to derive monthly SST anomalies
for the region extending offshore to 108°E (extent in Figure 4.2, see also (Pattiaratchi and Hetzel, 2020)). This was to reflect
the extensive duration (~9 months) of the pelagic larval and pre-settlement stage of *P. cygnus* (Phillips, 1981). All monthly
SST anomalies were originally included in the analysis due to the likely importance of temperature on all stages of
the pelagic larval stage (Caputi et al., 2001; de Lestang et al., 2015).

325 Altimeter data was accessed from the IMOS AODN (portal.aodn.org.au) to further investigate the
relationship between the PI and the energy the relationship between the puerulus index and energy in the system, in particular.
To investigate the long-term KE and EKE over the south-east Indian Ocean this data was applicable (Pattiaratchi and Siji,
2020)

3.3 Independent Breeding Stock Survey (IBSS)

330 Independent Breeding Stock Surveys (IBSS) have been conducted annually since 1992 over the last new moon (~ 15
November) before the start of the historic fishing season (de Lestang et al., 2018). The catch rates of spawning females from
this survey (adjusted for fecundity) provide a standardised standardized index of egg production egg production index. It is
conducted at up to 6 six sites spanning the fishery and close to the timing of peak of in egg production (November) (Caputi et
al., 1995; Chubb, 1991; de Lestang et al., 2016). Therefore, The IBSS was included in the our analysis, to account accounting
335 for for likely variability in the number of hatching larvae each season larvae.

3.4 Multiple regression analysis Generalized Additive Modelling

The oceanographic variables likely to influence water movement and the distribution and survivorship of *P. cygnus*,
detailed above, were considered as predictors of the puerulus settlement within a generalized additive model (GAM) multiple
340 regression analysis. In addition, the IBSS was included as a predictor to include variability in the number of hatching
larvae. Due to the large extensive latitudinal range of the settlement data, spatial variability of some environmental variables
was incorporated by were dividing them into northern, central or southern areas depending on the data type and availability
(Appendix 1). A value was obtained for each possible predictor variable to align with each half of the puerulus season.

All variables considered were examined to determine which could be treated as continuous covariates. Firstly, a linear
regression analysis was performed to assess whether there were strong (>0.870) correlations between any variable existed

345 ~~between variables. Where one was found valid, a case by case approach was taken to determine whether both, an average, or one of the two variables was to be included in the overall model prior to before the time series modelling, - this eliminated potential problems with collinearity and overfitting (Graham, 2009). Bottom temperatures were all highly correlated (>0.89) and therefore were therefore averaged to give a single variable. Co-correlation between the SST of adjacent months lead to a winter and summer average being used.~~

350 ~~Generalised-Generalized~~ additive models (GAMs) with full subset model selection (FSSgam) were used to investigate the influence of ~~the final~~ 16 different response variables, with the eight sites divided into early and late puerulus settlement periods (Fisher et al., 2018). ~~Predictors were originally limited to a maximum of three knots per spline, -h~~ However, due to the relatively small sample size and heterogeneous distribution of the predictors, cross-shelf transport remained as such, but other predictors were treated as linear relationships. ~~MM~~Models containing variable combinations with correlations > 0.4 were excluded, to eliminate potential problems with collinearity and overfitting (Graham 2003). Due to the relatively small sample size and heterogeneous distribution of the predictors, all were ~~treated as~~ limited to a linear relationships, except cross shelf transport, which was limited to a maximum of three knots per spline, and, ~~In addition, m~~model sizes were limited to three predictors to prevent overfitting. Model selection was based on Akaike's An Information Criterion (AIC, Akaike, 1973) ~~optimised-optimized~~ for small samples sizes (AICc, Hurvich and Tsai, 1989), ~~and~~ The best models were selected ~~at were~~ the most parsimonious within two AICc units of the model with the lowest AICc (Burnham and Anderson, 2002). Importance scores for each variable were obtained by summing the AICc weights of each model that each variable occurred within (Fisher et al., 2018).

The R language for statistical computing (R Core Team 2018) was used for all data manipulation (Wickham et al., 2018) (dplyr, Wickham et al. 2018) and analysis (Wood, 2017) (mgcv, Wood 2011). ~~In addition,~~ MATLAB and the m_map toolbox were used for any spatial plotting (MATLAB, 2019b; M_Map: A mapping package for MATLAB, Version 1.4m).

370 ~~All variables considered were examined to determine which could be treated as continuous covariates. Linear regression analysis was performed to assess whether there were strong (>0.80) correlations between any variable. Where one was found, a case by case approach was taken to determine whether both, an average, or one of the two variables was to be included in the overall model prior to the time series modelling. Bottom temperatures were all highly correlated (>0.89) and were therefore averaged to give a single variable. Co correlation between the SST of adjacent months lead to a winter and summer average being used.~~

375 The data for each oceanographic and meteorological variable were collated into annual values, ~~They and~~ resulted in a total of 39 possible predictors of the puerulus index ~~PI at sites for late~~ puerulus settlement (8 sites); and 33 possible predictors of the early puerulus settlement at sites (8) ~~for early settlement-~~ (Appendix A). LC strength in summer and ~~the~~ late CC strength predictors for early settlement were omitted since they occur after early settlement each season. Considering the large number of predictors and ~~in order to interpret~~ interpretation of the results, a hypothesis table including each predictor was made (Table

1). Given that the predicted data availability and the spawning season being-is in the calendar year prior, the relationship between all predictors and puerulus settlement was limited to the 2001 to 2017 seasons.

380 3.5 Exploration of oceanographic patterns

Findings of importance were expanded on from the results of the generalized additive model (GAM) analysis. Seasonal and inter-annual variability, not captured within the GAM, were explored. An extended period of low activity was experienced in the south-east Indian Ocean between 2001 and 2007 (Pattiaratchi and Siji, 2020). Given that processes in the ocean do not respond instantaneously, these 'hiatus' conditions were explored as a whole. ENSO information (SOI) and the Fremantle Mean Sea Level (FMSL) was obtained from the Bureau of Meteorology (Bureau of Meteorology, 2021a, b). Altimeter data was accessed from the IMOS AODN to investigate the relationship between the PI and the energy system, in particular, the long-term KE and EKE over the south-east Indian Ocean (Pattiaratchi and Siji, 2020).

The interactions between the CC and LC during the summer. During the summer, the interactions between the Capes Current and Leeuwin Current were also addressed (Pattiaratchi and Woo, 2009). First, the LC and CC summer period strengths were standardized for each season, and then the difference between the two was plotted alongside the early and late puerulus settlement levels.

395 **Table 1 Predictor variables and metrics used in multiple regression to investigate variability in puerulus settlement and subsequent hypothesis.** The subscript s identifies the relativity of a month to the puerulus settlement season (May - Apr) in question. $s - 1$ is within the season prior and $s + 1$ is after. -ve denotes negative relationship and +ve denotes and positive relationship.

Predictor variable	Metric used	Hypothesised Hypothesized relationship to puerulus settlement
Leeuwin Current (LC)	Southward strength of the current in Sverdrups (Sv) at northern, central and southern locations for three periods: 1. Larvae hatching / transport offshore (Dec _{s-1} - Feb _{s-1}). 2. Puerulus transport towards continental shelf (May _s - June _s) 3. Peak settlement (Dec _s - Feb _s).	1. -ve (all sites). 2. +ve (all sites). 3. -ve (north sites), +ve (south sites).
Capes Current (CC)	Northward strength of the current in Sv at a north, two central and a south location over two periods: 1. Larvae hatching / transport offshore (Sep _{s-1} - Nov _{s-1} (early) and Dec _{s-1} - Feb _{s-1} (late)) 2. Peak settlement (Sep _s - Nov _s (early) and Dec _s - Feb _s (late))	1. +ve (all sites) 2. +ve (north sites), -ve (south sites)
Kinetic and eddy kinetic energy	Kinetic and eddy kinetic energy of the south-east Indian Ocean in cm ² /s ² over a north and south area defined in Figure 4.2a. 1. phyllosoma offshore (Jan _{s-1} - Dec _s)	1. +ve (all sites)
Cross-shelf transport	Cross-shelf transport over the continental shelf (150 - 50 meters) in Sv over a northern, two central and southern latitudinal bins. 1. Larvae hatching / phyllosoma transport west (Sep _{s-1} - Mar _{s-1}) 2. Puerulus transport east (Apr _{s-1} - Sep _s)	1. Westerly (-Sv) +ve 2. Westerly (+Sv) -ve
Temperature	Water temperature over three periods. 1. SST summer (Sep _{s-1} - Mar _{s-1}) and SST winter (Apr _{s-1} - Aug _s) 2. Bottom temperature during spawning (40 - 60 m depth, Sep _{s-1} - Mar _{s-1}) 3. Top 100 m Early-stage phyllosoma. (Jan _{s-1} - Dec _s)	1. SST +ve (all sites) 2. -ve (all sites) 3. +ve (all sites)
Independent Breeding Stock Surveys (IBSS)	1. IBSS index for the spawning season	1. +ve (all sites)

3.5 Exploration of oceanographic patterns

400 Subsequent to the results of the multiple regression analysis, findings of importance were expanded upon from the results of the multiple regression analysis. Seasonal and inter-annual variability, not captured within the multiple regression analysis, were explored. An extended period of low activity was experienced in the south-east Indian Ocean between 2001 and 2007 (Pattiaratchi and Siji, 2020). Given that processes in the ocean do not respond instantaneously, these 'hiatus' conditions were explored as a whole. In particular, the hiatus conditions experienced in the south-east Indian Ocean (Pattiaratchi and Siji, 405 2020) and interactions between the CC and LC during the summer (Pattiaratchi and Woo, 2009). ENSO information (SOI) and the Fremantle Mean Sea Level (FMSL) was obtained from the Bureau of Meteorology (Bureau of Meteorology, 2021a, b) (Bureau of Meteorology, 2021a, b) (Figure 2). The interactions between the CC and LC during the summer were also addressed (Pattiaratchi and Woo, 2009). The LC and CC summer period strengths were standardised for each season, and then the difference between the two was plotted alongside the early and late puerulus settlement levels.

Field Code Changed

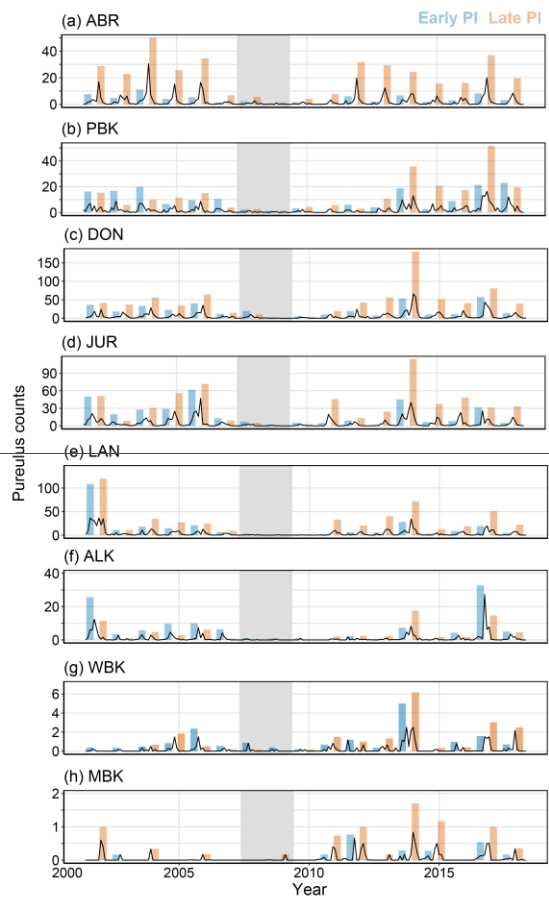
Formatted: Not Highlight

410 4 Results and Discussion

Results and discussion are combined into three sections (1) time-series patterns exploration of the spatial and temporal variability of the physical environment experienced by *P. cygnus* larvae settlement between 2000-2001 and 2017 and 415 associated oceanographic conditions experienced by the larvae to represent each puerulus settlement season (May to April) (when data was available); (2) exploring the correlation of oceanographic conditions with settlement data through a general additive model analysis; multiple regression analysis, and (3) inter-annual and seasonal oceanographic variability.

4.1 Time-series patterns

Puerulus settlement differs dramatically over the latitudes of the fishery, with central latitudes experiencing the highest numbers (Figure 4). At the Abrolhos (Figure 4a), the late settlement is consistently higher and remained consistent after the recruitment failure, which is expected (Kolbusz et al. 2021). Other sites, display similar early (Early PI) and late 420 (Late PI) puerulus settlements prior to before 2008. However, after 2009, recovery occurs predominately in the latter half (Figures 4a, c, d and e).



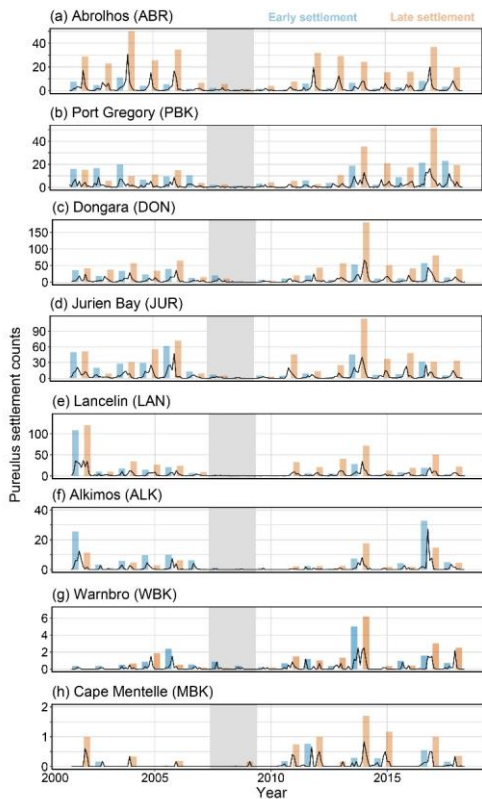
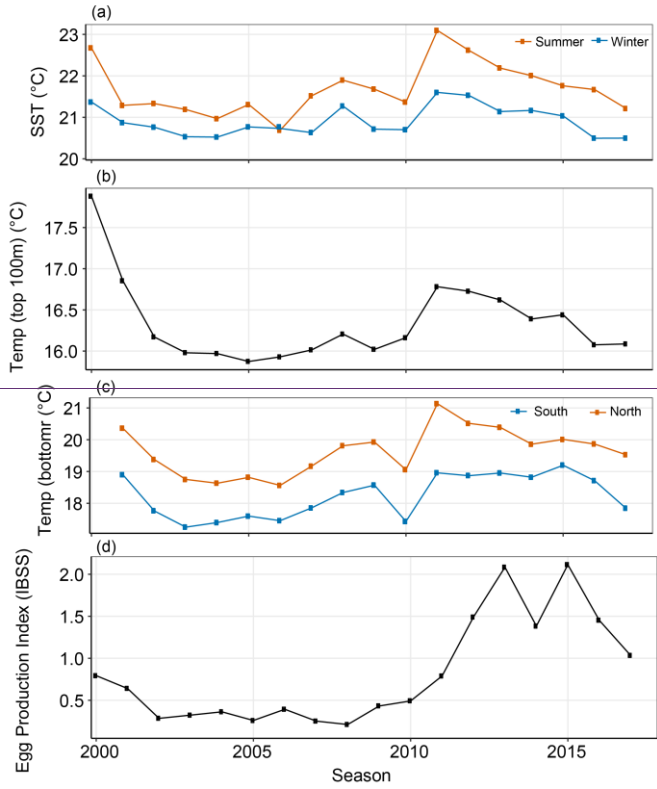


Figure 24 Monthly average puerulus counts for each monitoring site (black line) with the early (May - October, blue) and late (November - April, red) puerulus index settlement for the season. The index is a sum of the included monthly average puerulus counts. Grey shaded seasons (2008 and 2009) indicate the less than expected PI based on a priori relationships (Caputi et al. 2001).

The three temperature variables (SST, top 100 m temperature and bottom temperature) all followed a similar pattern to one another (Figures 5 a, b and c). They gradually decreased from highs in 2000 to a low in 2005 before slightly increasing from 2008, all reaching maxima in 2011 when a marine heat-wave occurred in February (Wernberg et al., 2012). There was a decrease of approximately 1-2-°C in bottom temperature during the spawning season was evident over the early 2000s, which shifted over the low PI seasons (grey seasons, Figure 5 a-c), and it then increased again by 2012 (Figure 5). Until the heatwave, the variation in PI at some sites (Lancelin and Port Gregory) additionally aligned with the SST fluctuations. This is

likely the bottom temperature variation captured by de Lestang et al. (2015). ~~There was no difference seen between the average bottom temperatures over the whole spawning season as opposed to only the start of the spawning season.~~ The winter months (June to August) had less than one degree of between year annual variability over the entire temporal scale.



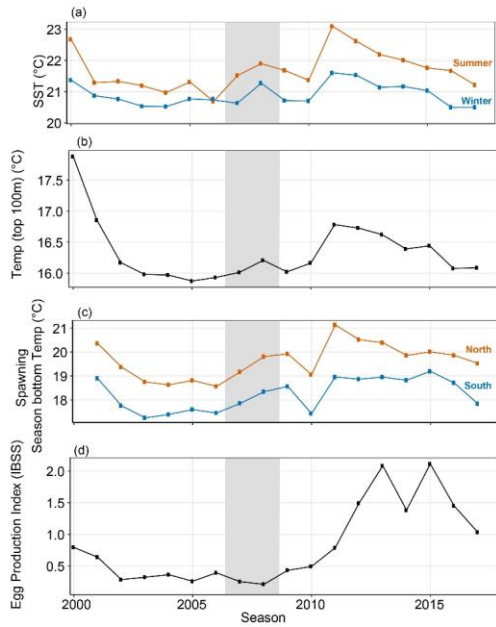


Figure 35

440 **Figure 5** Parameters calculated for seasonal analysis of puerulus index (PI) (a) Sea surface temperature (°C) from 24 - 34° S and
 445 out to 108° E obtained from the SSTAARS daily dataset on the IMOS AODN portal from 1996 to 2016; (b) Temperature in the top
 100 m of the offshore area from 24 - 34° S and east of 108°E over Jan - Dec, the average time phyllosoma are offshore (c) Average
 bottom temperature (40 - 80 m depths) (°C) of the spawning season (season - 1) for associated PI season for October to March in
 the northern (blue line, shown in Figure 4a2a) and southern latitudes (red line, shown in Figure 4a2a) of the fishery (d) The
 Independent Breeding Stock Survey Index (IBSS) lagged 1-one year to give a spawning stock index for the year prior (de Lestang et
 al. 2016). Grey shaded seasons (2008 and 2009) indicate the less than expected PI based on a priori relationships (Caputi et al. 2001).

The IBSS was consistently under 0.5 from 2002 until the 2011 season before increasing three-fold by 2013 to record-
 highs (Figure 45) (de Lestang et al., 2016). Previous studies have not found the IBSS to be implicated in the recruitment failure
 (de Lestang et al., 2015), but, However, it has been included in the current analysis for completeness and because studies
 of recruitment failures in other fisheries have frequently suggested spawning biomass to be a factor (Guan et al., 2019; Ehrhardt
 and Fitchett, 2010). In addition, the IBSS increased from 2011, this is suspected likely to be due to the restrictive
 fisheries management. After the lower than expected puerulus settlement in 2008 and 2009, restrictions to fishing were
 designed to preserve spawning biomass. Therefore the IBSS was expected to increase, designed to preserve spawning biomass,
 introduced after the recruitment failure.

455 The LC was the strongest over the winter months, reaching 7 Sv in the 2000 season at 34° S (Figure 6a). However,
the LC in summer LC was strongest in 2010, at 27° S. Both these values, which aligns values align with strong La Niña
conditions (Boening et al., 2012). This but does maximum, however, did not correspond to a maxima maximum in winter LC
strength (Figure 6b) (Wijeratne et al., 2018). The CC strength was highly variable between latitudes. Over the initial months
of the current CC forming (Figure 7a6c), it is, on average, strongest at 30° S. The CC displayed a roughly a similar pattern
460 across all latitudes with less variability in current at 27° S where it is weakest (Figure 76 c and d). CC minima occur over the
2010 to 2012 seasons in both the early and late strength signals (Figure 6 c and d). Spatial variations in the LC and CC were
clearly distinguishable with increased LC at the southern latitude (Figure 6 a and b) and the strongest CC signature at 30° S
(Figure 76d) as reported previously by Wijeratne et al. (2018).

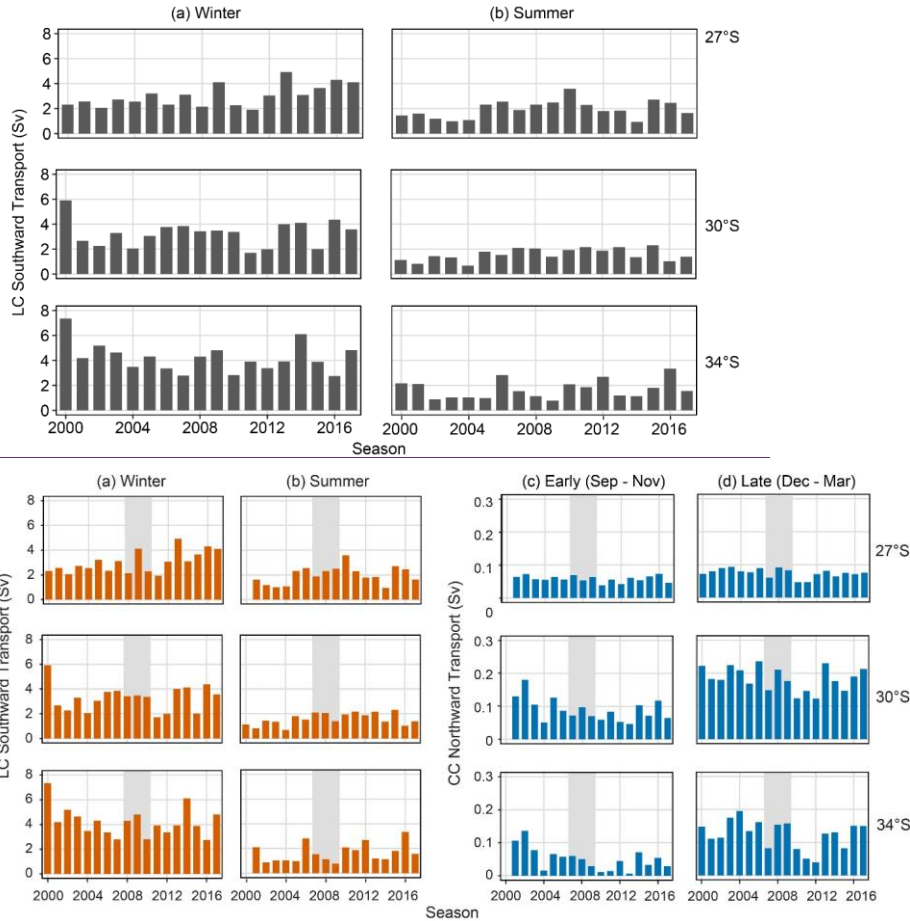


Figure 466 Leeuwin (LC) and Capes Current (CC) strengths at 27° S, 30° S and 34° S (a) The Leeuwin Current strength (southward transport, Sv) at 27° S, 30° S and 34° S over (a) winter (May - July) and (b) summer (December - February) (c) CC (northward transport, Sv) (c) over the early portion of the summer (September - October) and (b) late portion of the summer (December - March). Grey shaded seasons (2008 and 2009) indicate the less than expected PI based on a priori relationships (Caputi et al. 2001).

Water circulation ~~over-at~~ all latitudes of the fishery were predominantly driven by the LC with the changing topography down the coast causing less onshore flow on average within the centre of the fishery (29° S) (Rennie et al., 2007; Feng et al., 2010; Wijeratne et al., 2018). Regions with a wider continental shelf generally have higher retention of waters ~~therefore, therefore,~~ causing less cross-shelf transport of water. Depth-averaged cross-shelf transport of water was predominantly onshore at both 33°S and 29°S (Figure 87). This was not unexpected given the steep topography of the continental shelf and LC interactions. Average monthly variations in cross-shelf transport indicated that between April and September, onshore transport increased at 33°S and 29°S, however, decreased at ~~2931~~°S and 27°S (Figure 78). Coastal geographic features increase the spatial heterogeneity over the latitudes and ~~additionally,~~ how the LC interacts with the nearshore (Feng et al., 2010). ~~In particular a~~At 27°S, on average offshore transport was possibly due to more mixing and a wider continental shelf. ~~This and inerea is due to the topography of sed mixing around Shark Bay and with the contribution of the Ningaloo Current (Figure 42b), likely playing a role (Woo and Pattiaratchi, 2008).~~

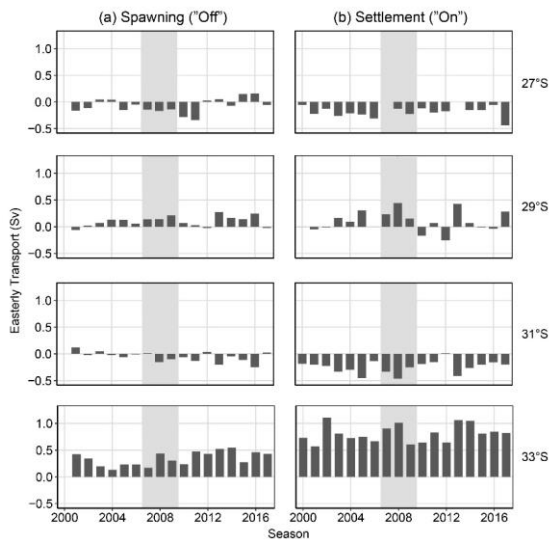
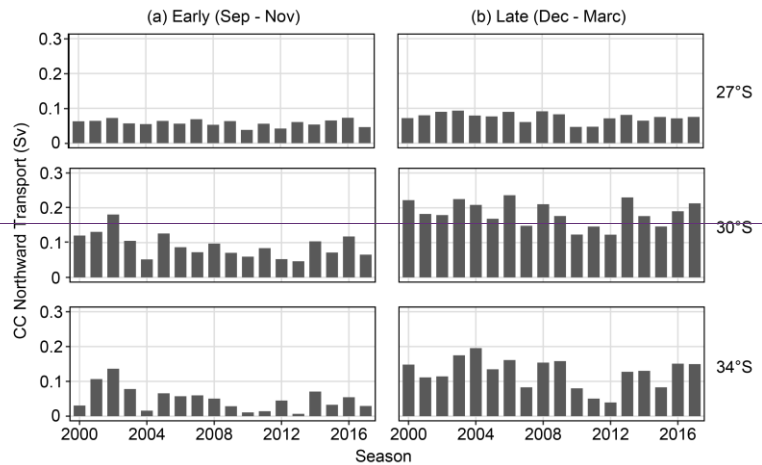
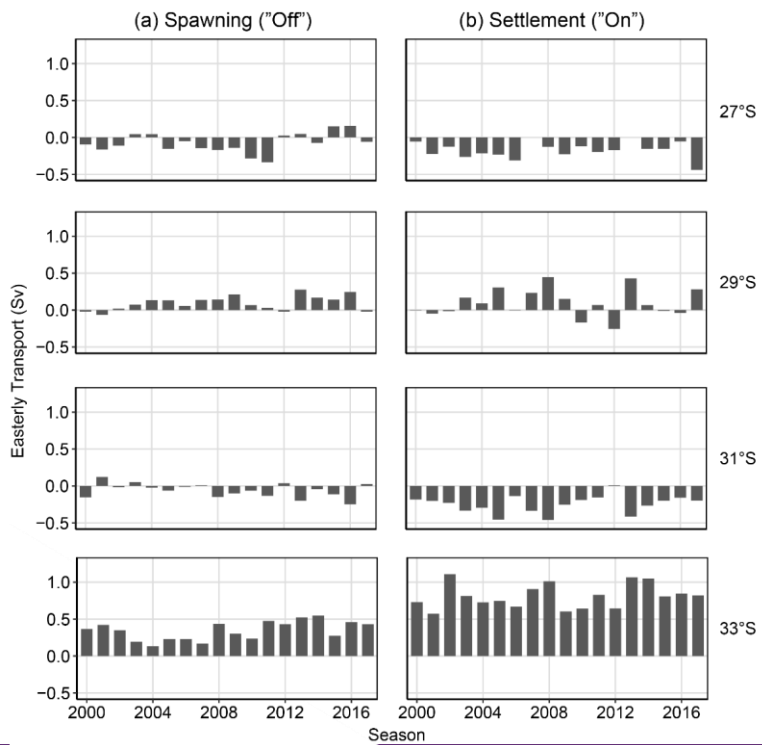


Figure 877 Cross-shelf transport (easterly) between 200 - 50 meters over 2-degree latitudinal bins (26-28° S, 28-30° S, 30-32° S and 32-34° S). Averaged for the (a) spawning "off" transport season (September-February, season -1) and (b) settlement "on" transport season when variation in cross-shelf transport is the highest (April-September). The Capes-Current strength (northward transport,

485

490 Sv) at 27°S, 30°S and 34°S over (a) the early portion of the summer (September – October) and (b) late portion of the summer
(December – March). Grey shaded seasons (2008 and 2009) indicate the less than expected PI based on a priori relationships (Caputi
et al. 2001).

495 Variations in EKE and KE over the time series show approximately 5-yearly patterns (Figure 8) in fluctuation with
maxima in 2000, 2005 and 2011 aligning with ENSO events (Pattiaratchi & Siji 2020). From 2002 to 2008, the KE and EKE
were relatively low, indicating a weaker LC over those seasons. Particularly over the southern box, the decrease in KE and
EKE and recovery by 2012 show similar patterns to the puerulus settlement (grey years, Figures 8c and d). Additionally, the
southern box shows increased variability, suggesting greater variability in the LC at southern latitudes (Figures 8c and d).
Conversely, the northern values, particularly for KE, increased over the same time frame, with less variability (EKE),
indicating that different forcing mechanisms, such as the South Indian Counter-Current, may play a role (Figures 8c and d).



500 - **Figure 8** Cross-shelf transport (easterly) between 200–50 meters over 2 2-degree latitudinal bins (26–28° S, 28–30° S, 30–32° S and 32–34° S). Averaged for the (a) spawning “off” transport season (September–February, season -1) and (b) settlement “on” transport season when variation in cross-shelf transport is the highest (April–September).

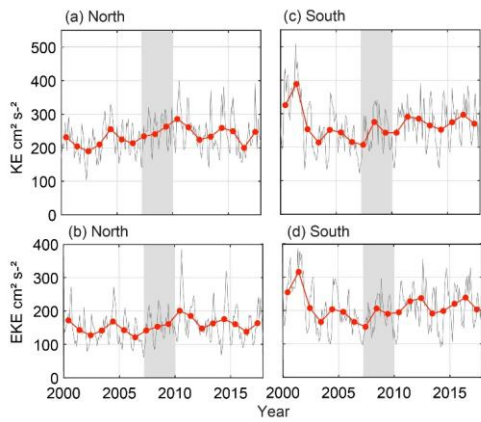
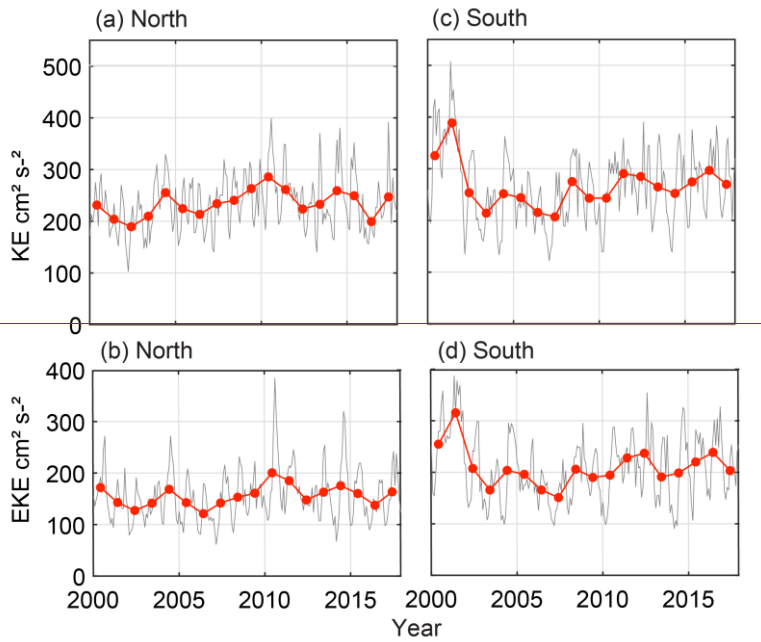


Figure 1098 Monthly kinetic energy and eddy kinetic energy (grey) with yearly averages (January-December) (red). North and south divide are shown in Figure 1a2a. (a) KE ($\text{cm}^2 \text{s}^{-2}$) in the north (b) EKE ($\text{cm}^2 \text{s}^{-2}$) in the north (c) KE ($\text{cm}^2 \text{s}^{-2}$) in the south (d) EKE ($\text{cm}^2 \text{s}^{-2}$) in the south. Grey shaded seasons (years 2008 and 2009) indicate the less than expected PI based on a priori relationships (Caputi et al. 2001).

Variations in EKE and KE over the time-series show approximately 5-yearly patterns (Figure 9) in fluctuation with maxima in 2000, 2005 and 2011 aligning with ENSO events (Pattiaratchi & Siji 2020). From 2002 to 2008, the KE and EKE were both relatively low, indicating a weaker LC over those seasons. The southern box (Figures 8c and d) had an increased variability suggesting there was a greater variability in the LC at southern latitudes. Whereas, over the northern box, there was a peak in 2010 which a peak in 2010 was more pronounced in the KE than EKE (Figure 9). Over From 2002 to 2008, the KE and EKE were both relatively low, indicating a weaker LC over those seasons.

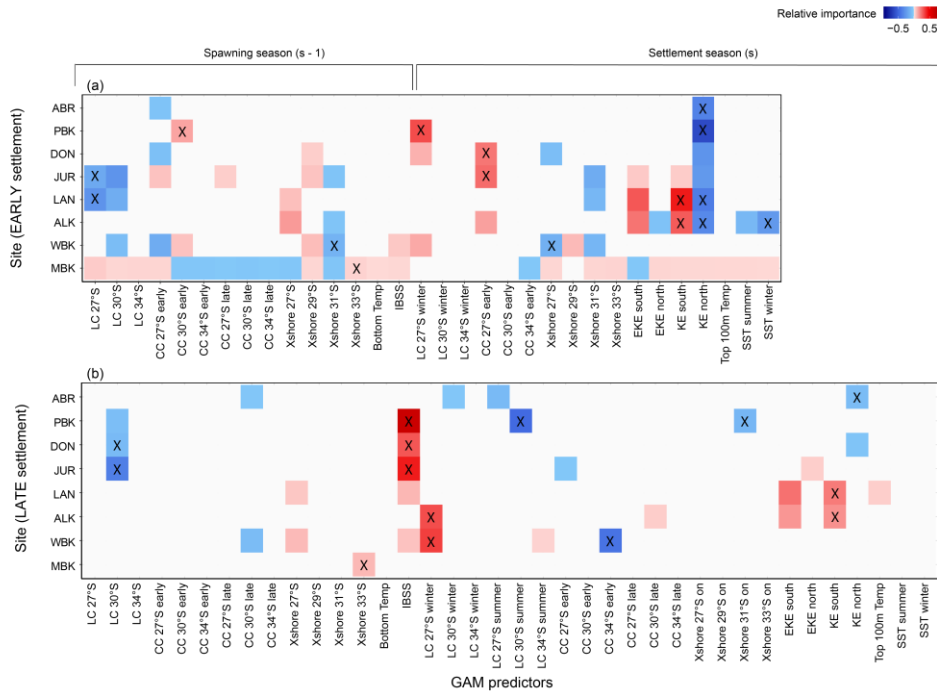
4.2 Multiple regression analysis Generalized Additive Model

The generalized additive model (GAM) analysis shows that puerulus settlement at adjacent sites tend to be influenced by similar oceanographic variables. However, the Abrolhos (northern-most and offshore) and Cape Mentelle (southern-most) sites are somewhat outliers (Figure 9, Appendix B). The most significant relationships did vary between the early and late portions of the seasons and between sites, as expected (Table 1). Those of note are discussed hereafter.

In contrast to our predictions (Table 1), sites were correlated by a negative relationship to KE in the north for early settlement (Figure 9a). This correlation was more robust for the northern sites. A strong KE implies a strong LC signature over the defined spatial area (Figure 2a). Comparatively, EKE and KE in the south had positive relationships to sites in the centre of the fishery for early and late settlement, suggesting a different forcing could be at play (Figure 9). This was alluded to within the time-series analysis (Figure 8). The possibility that two adjacent parts of the south-east Indian Ocean would have opposing effects on the settlement at only two locations appears spurious. However, the southern and central flows of the South Indian Counter Current (sSICC, cSICC) flow eastward within the southern and northern KE 'boxes' respectively (Menezes et al., 2014). These current jets connect with the LC and may cause the temporal and spatial difference in KE and subsequent influences on puerulus settlement. In particular, for the Abrolhos, KE in the north is within the most parsimonious model for early and late settlement. Due to the sites' location offshore, increased water movement may prevent puerulus from successfully settling on the islands within the defined area of KE. Instead, they could swim elsewhere with less resistance. This difference in KE relationships suggests different driving mechanisms over the fishery on both the temporal (early and late) and spatial (north and south) scale.

The Multiple regression analysis indicated that the factors which displayed the greatest most significant relationships with early settlement (Figure 10a), and were in line with our predictions (Table 1), were KE in the south (for two southern PI sites with some further importance at Lancelin and Alkimos), and both LC at 27° S during summer and early CC at 30° S for westward transport of phyllosoma (Jurien Bay, Lancelin (LC) and Port Gregory (CC)). These were in line with our predictions (Table 1). In addition, as predicted (Table 1), the LC in winter and CC over the early summer, both at 27° S,

540 during puerulus returning, had a positive relationship to coastal sites north of Jurien Bay, which was also predicted. Whereas for late settlement (Figure 10b), the dominant factors were the LC at 30° S during summer impeding the offshore transport of larvae, the IBSS, the LC at 27° S while puerulus were returning (Alkimos and Warnbro), and KE in the south at Laneclin and Alkimos.



545 Figure 11: Variable importance scores within 2 AIC of the top model from the multiple linear regression analysis (GAM) to predict the (a) early and (b) late settlement at sites. Full results are in Appendix Table B1 (early) and B2 (late). The timeline (above) indicates the timing of the variables from either the spawning season (s-1) where larvae are moving offshore (westward) and the settlement season (s) where larvae are moving eastward. Positive (red), zero (white) and negative (blue) relationships with variables are shown, and variables within the most parsimonious model for each site are indicated (X).

550

In contrast to our predictions (Table 1), sites were correlated by a negative relationship to KE in the north for early settlement. This correlation was stronger more robust for the northern sites. A strong KE implies a strong LC signature over the defined spatial area (Figure 1). Comparatively, EKE and KE in the south had positive relationships to sites in the centre of the fishery for early and late settlement, suggesting a different forcing could be at play (Figure 10). The possibility that two

555 adjacent parts of the south-east Indian Ocean would have opposing effects on the settlement at only two locations appears spurious. However, the southern and central flows of the South Indian Counter Current (sSICC, eSICC) flow eastward within the South and North Ke 'boxes' respectfully (Menezes et al., 2014). These current jets connect with the LC and may cause the temporal and spatial difference in KE and subsequent influences on puerulus settlement. South Indian Counter Current flows eastward within the defined southern 'box' of KE, one would expect if this had such an influence that it would be true for all sites and not only within the early portion of the season (Wijeratne et al., 2018). In particular, for the Abrolhos, KE in the north is within the most parsimonious model for early and late settlement. Due to the sites' location offshore, increased water movement may prevent puerulus from successfully settling on the islands within the defined area of KE. Instead, they could swim elsewhere with less resistance. This difference in KE relationships suggests different driving mechanisms over the fishery on both the temporal (early and late) and spatial (north and south) scale.

565 Interestingly, the LC during the spawning season at 27° S was within the most parsimonious model for Lancelin early settlement as a negative relationship (Figure 10a). This may be due to the LC being too strong for some early-stage phyllosoma to cross the shelf to the deeper ocean without being swept too far south for survival, this may explain why KE in the north is showing a negative relationship. LC at 27° S over the spawning season, KE in the north and EKE in the south are the only few parameters where similar patterns occur in the early and late settlement (Figure 10 a & b). In particular, for the Abrolhos, KE in the north is within the most parsimonious model for early and late settlement. Due to the sites' location offshore, within the defined area of KE, it is possible that increased water movement prevents puerulus from successfully settling on the islands and instead they are transported or swim elsewhere with less resistance.

575 The model results provide some clues regarding the influence of the LC and CC (LC winter, LC summer, CC early and late) on phyllosoma when they are in later-life stages. Interestingly, the LC during the spawning season at 27° S was within the most parsimonious model for Lancelin early settlement as a negative relationship (Figure 10a). Thus, for Lancelin, the LC may have been too strong for some early-stage phyllosoma to cross the shelf, to get westward, without being swept too far south for survival. Especially given the steep continental shelf at this latitude. A stronger LC in winter. In winter, a stronger LC (puerulus reaching the continental shelf) and a stronger CC (puerulus settling on reefs) were good-suitable for early settlement at Dongara. This was a hypothesised-hypothesized result (Table 1) and was also consistent at adjoining sites (Port Gregory for LC and Jurien Bay for CC, Figure 10a9a) (Pearce and Pattiaratchi, 1999). However, for later settlement, the opposite relationships occur. The LC in summer has a negative relationship to Port Gregory (and Abrolhos), and the CC has a negative relationship to Warnbro (Figure 10b9b).

585 As expected, northern sites (Port Gregory) are negatively influenced by the southward-flowing current (LC), transporting puerulus further southward. Similarly, southern sites are negatively influenced by the northward-flowing current (CC), transporting puerulus northward. However, these trends become vague over the central latitudes of the fishery where little to no relationships are found, especially during the summer of hatching (Figure 10a9a, CC 27° S early). This draws attention to the spatial and oceanographic heterogeneity of the study sites. Given the mix of both expected and unexpected and

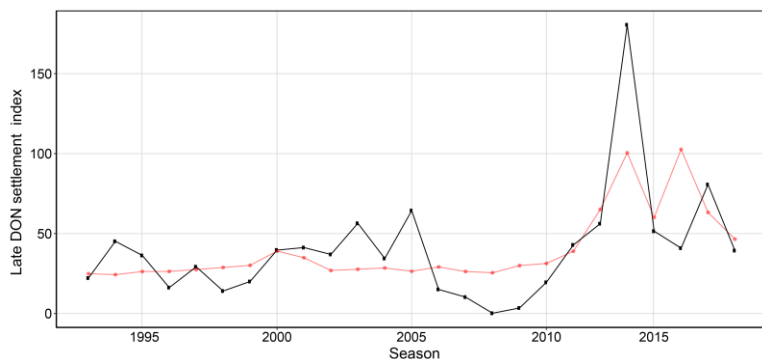
Field Code Changed

590 ~~strong and weak results from the multiple regression analysis, particularly for the early settlement, it is clear complex forcing's~~
are at play in the system, with both currents flowing in opposing directions perpendicular to the direction puerulus are swimming. The influence of factors found to have the strongest correlation on puerulus settlement is presented in the following
section (4.3).

595 ~~These results are in line with our predictions, with a northern site (Port Gregory) being negatively impacted by a~~
~~strong LC causing southward advection and a southern site (Warnbro) being negatively impacted by a strong CC transporting~~
puerulus northward, but these trends becomes vague over the central latitudes of the fishery where little to no relationships are
found, especially during the summer of hatching (Figure 10a, CC 27° S early). This draws attention to the spatial and
oceanographic heterogeneity of the study sites. Given the mix of both expected and unexpected and strong and weak results
from the multiple regression analysis, particularly for the early settlement, it is clear complex forcing's are at play in the
system, with both currents flowing in opposing directions perpendicular to the direction puerulus are swimming. The influence
600 of factors found to have the strongest correlation on puerulus settlement is presented in the following section (4.3).

The IBSS shows a strong positive relationship with Port Gregory, Dongara, Jurien Bay, Lancelin and Warnbro over
the late settlement, ~~h~~. However, ~~it~~ has little relationship with the early settlement (Figure 10-9 a and b). ~~These positive~~
~~relationships however, do corroborate that the egg production has an influence on~~ Nevertheless, these positive relationships
corroborate that the egg production influences the amount-number of larvae returning to the coast as puerulus and may more
605 accurately represent the spawning stock of puerulus reaching the coast over the latter half of the settlement season. Given the
longer time series available for the IBSS and Dongara settlement, we ~~reanalysed-reanalyzed~~ the relationship- for a more
~~extended period~~and. We found that pre-2000 that IBSS is a reasonable predictor with an R^2 of 0.434 and explaining 30.3% of
the deviance in the Dongara settlement (Figure 1+10). In an ideal scenario, one would expect all sites, both early and late, to
have a ~~position-relationship to-with~~ the spawning stock. For locations where increased IBSS did not ~~have a positive~~
610 ~~correlation~~positively correlate with PI, it may be solely that the influence of oceanographic factors on the puerulus settlement
was ~~higher~~more substantial.

Cross-shelf transport shows ~~sporadic-irregular~~ patterns between the sites. Cross-shelf transport for the spawning
season (27° S, 29° S and 33° S, Figure 9a) has some positive links to increased settlement in the early half of the season for
615 sites south of Dongara. However, this is the opposite for 31° S (Figure 10a9a), but these relationships are less pronounced over
settlement later in the year (Figure 10b9b). Various transportation pathways are likely working in opposing directions to
influence settlement at different locations. Average cross-shelf transport has previously indicated a break over the ~~mid-mid-~~
latitudes of WA (Wijeratne et al, 2018, Figure 109).



620 Figure 12410 Observed (black) and modelled (red) late Dongara (DON) settlement index from 1993 to 2018. The red line is the model most parsimonious model extended to 1993.

On an annual timescale, increased strength in KE in the northern offshore areas of the fishery (Figure 1) were associated with a decrease in puerulus settlement in the early portion of the season. It is not uncommon for the advective behaviour of large-scale eddies to negatively affect crustacean species (Medel et al., 2018; Nieto et al., 2014). Retention and dispersal of larvae can also differ in persistent eddy scenarios where a more uniform shape likely leads to retention but, However, a more eccentric shape leads to dispersal (Cetina-Heredia et al., 2019b). From our analysis we have not defined directionality and size of the LC eddies, but is an important consideration that would require further modelling, outside the scope of the current study. Earlier studies however, suggest an increase in the number of eddies positively influence the retention of larvae and, therefore, transport across the shelf and to the nearshore (Griffin et al., 2001; Yeung et al., 2001; Cetina-Heredia et al., 2019a, 2015). This is contradictory to our results. Here, Our study we have used the mean annual KE over a large spatial area, and the site in question is north of the highest density of puerulus settlement. By using a large spatial area we have omitted the influence of sub-mesoscale features within the region which could impact a puerulus. Using a large spatial area, we have omitted the influence of sub-mesoscale features within the region, which could impact a puerulus's ability to cross the shelf and reach coastal habitats (Cosoli et al., 2020).

635 These The GAM analyses suggest not only that PI at each site is influenced by different environmental drivers, but this also varies depending on when puerulus are returning that different environmental drivers influence PI at each site, but this varies depending on when puerulus returns to shore (early or late, Figures 10-9, 109a and 109b). However, we can establish discernible patterns with some certainty and physical relevance. Sites closer in latitude have similar results, Abrolhos and Cape Mentelle being the exception. Abrolhos is located off the shelf and has historically had different trends in PI compared to other locations and even on the adjacent coast. Also, since the recruitment failure of 2008 and 2011-09, The Abrolhos PI has also recovered to pre-failure levels, whereas coastal locations have not, in particular particularly at Lancelin and locations further

south, ~~the late season settlement has not recovered~~ (Kolbusz et al., 2021). Cape Mentelle has historically had a low settlement and also has a unique location being the farthest south. Early settlement at Cape Mentelle also had little difference between all top models within 2 AIC of the most parsimonious model (~~Cross~~cross-shelf transport at 33° S during spawning season). Despite one variable having the highest importance and being in the top model, there was little difference between all models within 2 AICc units. ~~Jurien Bay and Lancelin have similar results within the early settlement, but not later settlement.~~

Given the several months over which lobster larvae hatch, followed by their prolonged pelagic life cycle and settlement estimated to occur some 9-11 months later (Phillips, 1981), the large amount of variation and lack of ~~strong-solid~~ relationships between environmental or biological predictors and PI was not unexpected (Figure 2). However, we have revealed patterns up and down the coast, suggesting that both biological and environmental predictors can have a strong and sometimes consistent influence on puerulus settlement for adjacent sites.

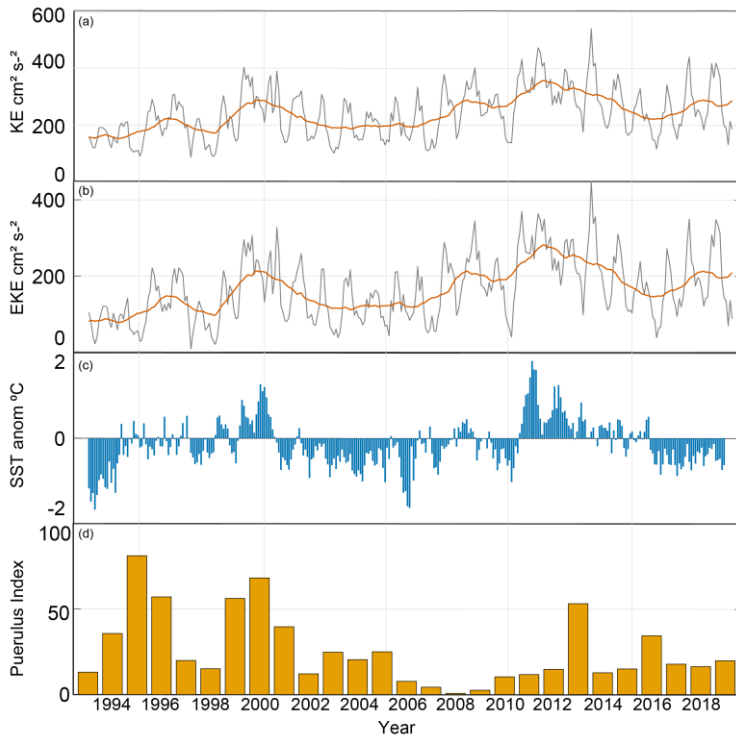
4.3 Variation in oceanographic conditions

All the oceanographic factors examined here have been suggested to ~~have a direct influence on~~indirectly influence *P. cygnus* larvae at some point in their first year of life. ~~However, (The forcing and interactions between these environmental variables over time~~Over time, ~~the forcing and interactions between these environmental variables~~ were too complex to examine in the ~~above~~multiple regression analysis ~~but~~. ~~However, they~~ may have as much influence on successful puerulus settlement as ~~opposed to~~instantaneous values used. ~~Furthermore, ver the large area of the fishery,~~ the various oceanographic mechanisms are ~~acting~~ differently, sometimes in competition (Figures 9a and b), to provide contrasting results for the different sites. ~~For this reason, u~~Using the ~~results of the above multiple regression analysis~~above multiple regression analysis results as an exploratory tool, we have additionally drawn upon patterns in the south-east Indian Ocean and WA coastal zone over the last two decades. ~~This includes as complementary~~ lagging conditions, ~~which~~ alongside the fishery changes, that may have contributed to the “~~worst-worst~~-case scenario” and resulted in the recruitment failure in 2008 - 2009.

4.3.1 Inter-annual: Hiatus period and cross-shelf transport

Over the past 30 years, links between ENSO events and the ~~puerulus index (PI)~~PI have been well documented ~~through~~ using the SOI (Figure 3) (Caputi et al., 2001; Pearce and Phillips, 1988). Warmer temperatures are experienced during stronger LC conditions evident during the La Niña phase (positive SOI), providing better conditions for larval development. The SOI record since these relationships began highlights the possibility of sustained neutral ENSO conditions to be a reason for this breakdown (Pattiaratchi and Hetzel, 2020; Pattiaratchi and Siji, 2020). From 2000 until 2009, ~~both a moderate La Niña phase~~ ~~neither a moderate La Niña phase nor a moderate El Niño phase occurred,~~ and consequently, the energy in the system also decreased (Figure 3). After 2009, an unusually strong LC (La Niña, 2011) was preceded by an unusually weak year (El Niño, 2010) (Huang and Feng, 2015). ~~Prior to~~Before 2008 there were fluctuations in LC strength, or phases of a moderate strength, over several seasons whilst the puerulus settlement also fluctuated ~~is a similar fashion~~similarly (Figure 3, and Caputi et al., 2001, Figure 56). An extended period (> 5 years) of low or neutral ENSO conditions, ~~termed a hiatus,~~ had not yet been

675 experienced since puerulus collection began; therefore, the relationship breakdown is not surprising. Recovery in puerulus numbers began after the strong La Niña in 2011, taking a few seasons to reach levels ~~prior to before the hiatus~~2000. If these strong La Niña conditions had not occurred, what would have been the response? Whether this 'delayed' recovery was due to ~~the climate inertia in memory in~~ the system adjusting or ~~the changes in recruitment numbers after changes in there~~ recovering after management changes to fishing the spawning stock ~~is, increasing the IBSS is unsure~~uncertain.



680 **Figure 131211 (a) Kinetic energy and (b) eddy kinetic energy ($\text{cm}^2 \text{s}^{-2}$) from altimeter data, the (c) SST ($^{\circ}\text{C}$) anomaly from SSTAARS and (d) Puerulus Index PI for the whole Western rock lobster fishery.**

685 Similarly, SST anomalies (Figure 1211) have periods of neutral conditions and ~~below below~~-average temperatures, respectively, from approximately 2000 to 2008 (Pattiaratchi and Hetzel, 2020). ~~It is possible that these extended low activity conditions~~These extended low activity conditions may have caused a shift in the conditions experienced by pelagic western rock lobster larvae. The patterns may be due to atmospheric and oceanic processes that imprint themselves upon the SST field.

The thermal energy of the ocean's thermal energy is communicated-transferred to the atmosphere via the sea surface, which is controlled by the SST-the SST controls. T-and thus, SST on a spatial scale plays a key-crucial role in regulating climate and variability. The extended period of cooler SST anomalies may have contributed to the low 2008 and 2009 settlements. A decreasing PI over the start of the century was in line with these patterns. Then recovery followed-and then recovery-post- the maxima experiences with the 2011/12 La Niña (Boeing et al., 2012), which perhaps took the system some years to return to conditions as normal-usual. It-Thus, it may not be a season-season-specific factor which-that has caused the years of low settlement in the late 2000s, but- Instead, consecutive years of these 'hiatus' conditions (Figure 1211) which have driven a regime shift in the environment impacting *P. cygnus* pelagic life stages (DeYoung et al., 2004).

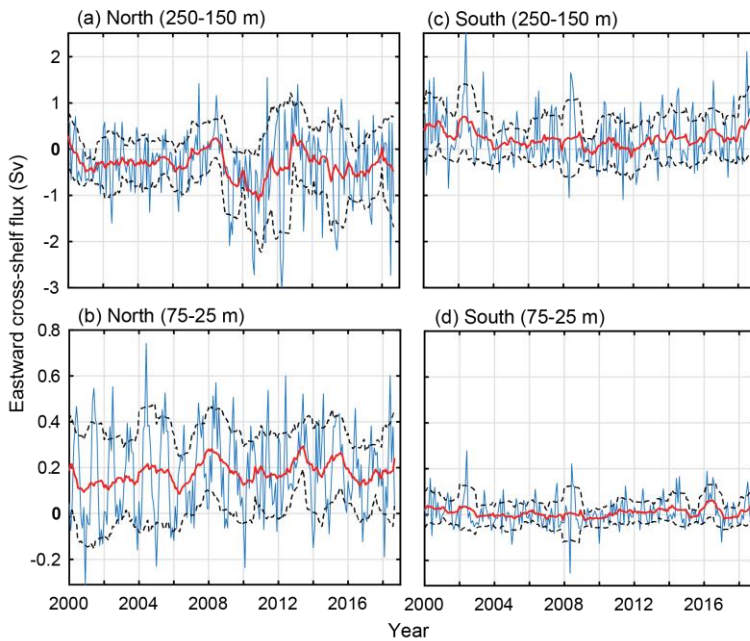


Figure 141312 Cross-shelf transport (easterly) between 2000 and 2018 off the shelf. North and south divide are shown in Figure 1a. (a) North cross-shelf flux between 250-150 m and (b) 75-25 m. (c) South cross-shelf flux between 250-150 m and (d) 75-25 m. The yearly moving mean (red) and with the positive and negative moving standard deviation (dashed black) are included.

The lack of statistical relationships with cross-shelf transport, Despite it being cross-shelf transport undoubtedly being a forcing mechanism behind larval transport into the nearshore, there was a lack of statistical relationships a lack of statistical relationships was found through the multiple regression analysis was unexpected. Given This is especially cause for

705 ~~further investigation since~~ the ‘hiatus’ conditions or shift after 2008 in the LC, one would expect some form of accompanying change in cross-shelf flux (Pattiaratchi and Hetzel, 2020). Over the 50 metre contour, there ~~is-are~~ no noticeable inter-annual changes over the 18 years between the south or north ~~binsboxes~~. In the south, there is ~~less-minor~~ variation in the standard deviation from the mean (Figure ~~4312~~, dashed lines); however, it is predominantly onshore transport on the shelf (50 m) and over the continental shelf (200 m). The cross-shelf transport in the north shows a ~~clearn~~ apparent increase in variability over the continental shelf (Figure ~~4312~~, 200 m) after 2008, highlighting the increased movement in water over the northern part of the fishery (Figure ~~4312~~). This is also where the LC increases over the summer ~~period~~ (Figure 5b); and a shift in puerulus settlement occur~~puerulus settlement shifts~~.

710 4.3.1 Seasonal: Capes Current and Leeuwin Current interactions during summer

715 ~~A shift in mean LC and CC conditions early in the season (late austral spring) has occurred subsequent to the recruitment failure. Prior to~~Before 2008, conditions were fairly-reasonably neutral over the early settlement season, leading to high/low puerulus settlement ~~to be~~ potentially controlled by oceanographic and/or biological factors (Figure ~~4413~~). Since 2009, the LC dominates conditions are such that LC dominating (blue years skewed to the right, Figure ~~4413~~), possibly causing ~~could give rise to~~ average to low puerulus conditions across all sites, E~~except at for~~ Cape Mentelle, the southern-most site and where higher settlement was experienced during these seasons, where Cape Mentelle is the most southern of the sites and potentially most isolated from the LC (Figure 14h). Comparatively, over the late period of settlement (Figure 154), the system ~~is dominated by the~~ CCCC dominates the system, with higher settlement occurring later in the summer (Figure 15). Thus, the years of recruitment failure ~~both~~ have neutral conditions where neither the CC nor LC is particularly dominant over the latter portion of the season. The same exists for 2007 and 2008 during the early portion of the season. Interestingly, during these recruitment failure years, the spatial extent of the LC during spring months (~~early settlement~~) was ~~also larger~~more considerable or on par with the ~~6 six~~ months prior, ~~during time~~ when newly hatched phyllosoma transport across the shelf into the open ocean may have also been impacted (Huang and Feng, 2015).

725 These patterns suggest that perhaps a timing mismatch is in play, suggested previously by de Lestang et al. (de Lestang et al., 2015). An increased LC while puerulus are crossing the shelf~~While puerulus are crossing the shelf, an increase in LC strength may transport them past southward and either settling closer to Cape Mentelle, away from suitable habitats or wash them too far offshore to return.~~ In contrast, a strong CC is likely to assist transport northward along the shelf, hence the increase in increasing settlement over the later part of the~~increasing settlement over the later season.~~ Interaction between these two ~~important~~critical currents over the shelf is clearly influencing~~influences~~ the movement of puerulus onshore and needs to be investigated in greater detail. Particle tracking modelling over these months would be a possible way to investigate these interactions; however, this is beyond the scope of the present study.

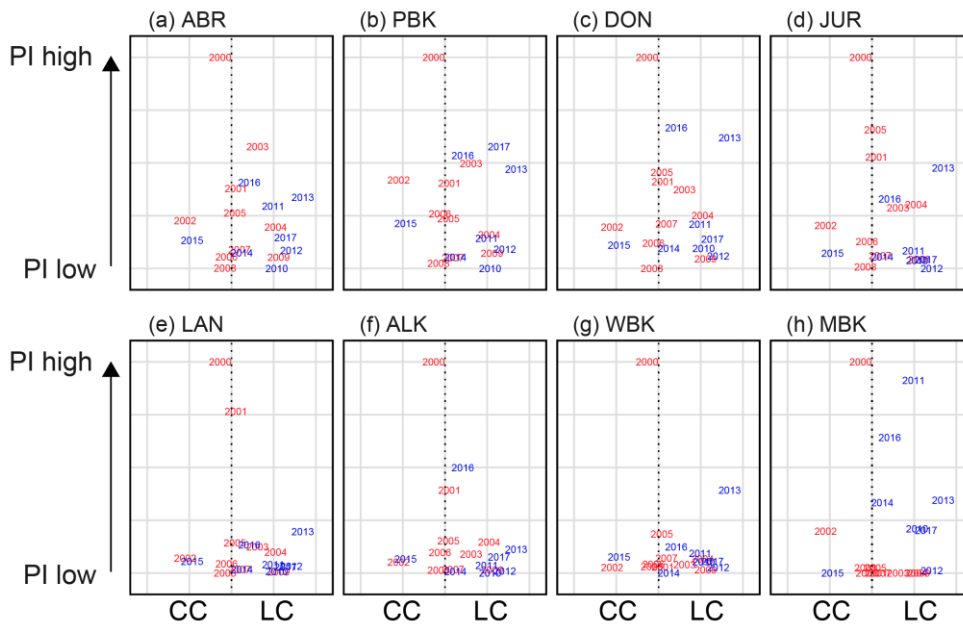


Figure 51514 Relationship of the more dominant current during the late-early spring/early summer (September - November) to early PI at monitoring sites (a) Abrolhos (b) Port Gregory (c) Dongara (d) Jurien Bay (e) Lancelin (f) Alkimos (g) Warnbro and (h) Cape Mentelle. The x-axis is the difference between the LC and CC standardized standardized, providing an indication of which is more prominent at the time. Red indicates the seasons before the recruitment failure, blue indicates seasons after.

735

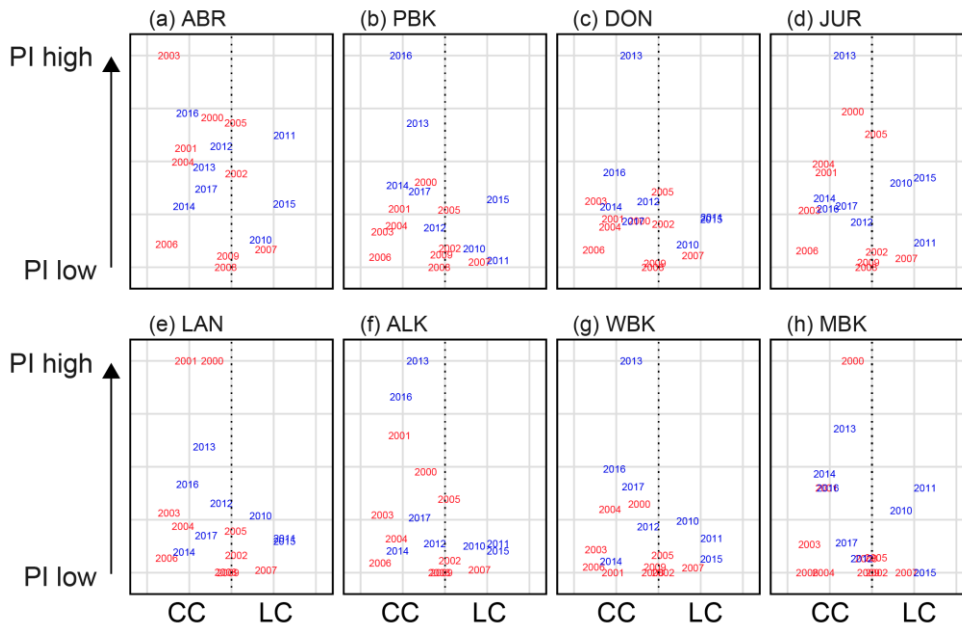


Figure 6: Relationship of the more dominant current during the late summer/early autumn (December - March) to late PI at monitoring sites (a) Abrolhos (b) Port Gregory (c) Dongara (d) Jurien Bay (e) Lancelin (f) Alkimos (g) Warnbro and (h) Cape Mentelle. The x-axis is the difference between the LC and CC ~~standardised~~ ~~standardized~~, providing an indication of indicating which is more prominent at the time. Red indicates the seasons before the recruitment failure, blue indicates seasons after.

These patterns suggest that perhaps a timing mismatch is in play, suggested previously by de Lestang et al. (de Lestang et al., 2015). An increased LC while puerulus are crossing the shelf may transport them southward and either settling closer to Cape Mentelle or wash them too far offshore to return. In contrast, a strong CC is likely to assist transport northward along the shelf, hence the increase in settlement over the later part of the season. Interaction between these two important currents over the shelf is clearly influencing the movement of puerulus onshore and needs to be investigated in greater detail. Particle tracking modelling over these months would be a possible way to investigate these interactions, however this beyond the scope of the present study.

5 Conclusions and Implications

The objective of the current study was to determine oceanographic and biological factors that may explain the previously unexplained failure of puerulus settlement (2008-2009) and subsequent change in the proportions of puerulus settling in early

vs late parts of the season (Kolbusz et al., 2021). The ~~study~~ was completed through an exploratory multiple regression analysis encompassing direct oceanographic and biological factors likely to influence the pelagic early-life cycle of *P. cygnus*.

755 The main conclusions were as follows:

- Local oceanographic and biological conditions greatly influence ~~the settlement of~~ *P. cygnus*, as settlement of puerulus at adjacent sites along the coast tend to be influenced by similar oceanographic and biological variables. ~~Offshore. This is also true for the offshore the~~ Abrolhos Islands, ~~which~~ had a unique yet consistent pattern of settlement that correlated with particular oceanographic and biological factors.
- On a fishery-wide scale, the period of recruitment failure (2008 and 2009) and the associated low settlement period (2004 – 2010), coincided with a ~~period of hiatus~~ hiatus period in the Leeuwin Current system. This was associated with mainly neutral ENSO conditions and slightly cooler SST anomalies.
- Increased KE in the northern region of the fishery was negatively correlated to puerulus settlement in the early period of the season, whilst the KE (and EKE) in the southern region was positively correlated at selected sites. This suggests different driving mechanisms over the whole range of latitudes that encompass the fishery for settlement early and later in the season.
- Seasonal variation of the LC system likely controls the conditions that favour increased puerulus settlement. ~~A strong LC during the summer months of hatching. During the summer months of hatching, a strong LC~~ negatively affects puerulus settlement at central sites after their pelagic phase. During the subsequent winter, the system is dominated by a strong southward LC and its associated eddies, which then assists onshore phyllosoma transport. Then, whilst the newly metamorphosed puerulus are moving onshore across the LC, should it be too strong, the current can negatively impact settlement at the northern sites but positively impact the southern sites.
- An increase in the strength of the LC in the summer months since 2006, combined with a decrease in the strength of the CC over the early summer months, may have caused a timing mismatch for puerulus settling on nearshore reefs. If the LC ~~was were~~ stronger in summer, a strong CC would be needed to counteract the southward flow to get the puerulus transported northward, which has occurred in recent years. ~~However, the~~ CC in the latter half of the summer ~~however,~~ has been less variable and ~~has~~ not declined to the same extent, potentially explaining the trend of ~~greater better~~ settlement later in the season.
- Between 2008 and 2011, the cross-shelf transport in the northern half of the fishery across the continental shelf became more variable whilst consistently offshore. This overlap with the period of recruitment failure suggests that cross-shelf transport in an offshore direction could have reduced the transport and subsequent settlement of puerulus onshore.

780
785 These findings have implications for fisheries management and their modelling of future stocks of catchable western rock lobsters. ~~Where environmental conditions are suspected to alter of altering the puerulus settlement, these~~ Environmental

conditions are suspected of altering the puerulus settlement, which can be incorporated in planning and management. For example, reductions in the fishing effort can encourage an increase in larvae for the following season (de Lestang et al., 2015).

790 Despite its exploratory nature, this study offers insight into factors potentially behind the recruitment failure ~~which have not been addressed prior~~that have not been addressed before. It also expands our current understanding of what oceanographic variables potentially influence puerulus settlement and how the variables themselves are intertwined in this complex system. With the available numerical modelled data ~~we are able to, we can~~ show that it is not solely the LC ~~which that~~ is the dominating factor behind puerulus settlement variability but the CC, cross-shelf flow ~~and the state of the system,~~ and the system's state as a whole.

Table A1. Oceanographic data sources and sites used to calculate the 40 predictor variables included in time series analysis. Unless stated, the timing is within the season of puerulus settlement. Spawning season indicates that the variable is from the year prior or within the spawning season as larvae hatch.

Predictor Variable	Data source	Northern	Central	Southern	No. Variables	
Leeuwin Current strength (Austral winter mean)	ozROMS	27°S	30°S	34° S	3	
Leeuwin Current strength (Austral summer mean) Spawning season	ozROMS	27°S	30°S	34° S	3	
Leeuwin Current strength (Austral summer mean)	ozROMS	27°S	30°S	34° S	3	
Capes Current strength (Austral spring mean)	ozROMS	27°S	30°S	34°S	3	
Capes Current strength (Austral summer mean)	ozROMS	27°S	30°S	34°S	3	
Capes Current strength (Austral spring mean) Spawning season	ozROMS	27°S	30°S	34°S	3	
Capes Current strength (Austral summer mean) Spawning season	ozROMS	27°S	30°S	34°S	3	
Cross-shelf transport – offshore (spawning season) 150 – 50 m (September - March mean)	ozROMS	26-28°S	28-30°S	30-32° S	33-33°S	4
Cross-shelf transport – onshore 150 – 50 m (April - September mean)	ozROMS	26-28°S	28-30°S	30-32° S	33-33°S	4
Bottom temperature (October - March) Spawning season	ozROMS	24.5-30.5°S		30.5-34.5°S	2	
EKE (January – December mean)	ozROMS	24.5-30.5°S		30.5-34.5°S	2	
KE (January – December mean)	ozROMS	24.5 - 30.5°S		30.5-34.5°S	2	
SST October – March mean (summer) April - September mean (winter)	SSTARS, Integrated Marine Observing System (IMOS, oceancurrent.imos.org.au) Australian Ocean Data Network (AODN) portal (portal.aodn.org.au) (Wijffels et al. 2018)	WA waters extent 21°S-36°S 108°E to coastline			2	
Temperature in the top 100 m	ozROMS	WA waters extent 21°S-36°S			1	

(January – December mean)		108°E to coastline	
Independent Breeding Stock Survey (IBSS) Spawning season	DPIRD	Index for whole fishery	1
Total predictor variables			39

800 **Table A2. Top generalised additive models (GAMs) for predicting the early puerulus settlement at the eight sites from full subset analyses. Difference between lowest reported corrected Akaike Information Criterion ($\Delta AICc$), $AICc$ weight ($\omega AICc$), variance explained (R^2) and effective degrees of freedom (EDF) are reported for model comparison. Model selection was based on the most parsimonious model (fewest variables) within two units of the lowest $AICc$, and models are ordered by parsimony.**

Site	Model	$\Delta AICc$	$\omega AICc$	R^2	EDF
Abrolhos	KE North	0	0.032	0.30511	2
	CC 27° S early + KE North	1.98	0.012	0.33571	3
Port Gregory	CC 30° S early (spawning season) + KE North + LC 27° S winter	0	0.06	0.64656	4
Dongara	KE north + LC 27° S winter	0.668	0.043	0.56042	3
	CC 27° S early	0	0.017	0.24911	2
	KE north	0.584	0.012	0.24508	2
	CC 27° S early + KE north	0.933	0.01	0.34984	3
	KE north + LC 27° S winter	1.523	0.008	0.43133	3
	KE north + Xshore 29° S (spawning season)	1.677	0.007	0.42171	3
	CC 27° S early + Xshore 27° S	1.843	0.007	0.30153	3
	CC 27° S early + LC 27° S winter	1.939	0.006	0.35149	3
	CC 27° S early + LC 27° S (spawning season)	0	0.018	0.37311	3
	CC 27° S early + CC 27° S late (spawning season) + KE north	0.071	0.017	0.41751	4
	CC 27° S early + LC 30° S (spawning season)	0.373	0.015	0.36202	3
	KE north + Xshore 31° S	0.408	0.015	0.41185	3
Jurien Bay	KE north + LC 30° S (spawning season) + Xshore 29° S (spawning season)	0.877	0.012	0.52731	4
	KE South + LC 30° S (spawning season) + Xshore 29° S (spawning season)	1.186	0.01	0.59535	4
	CC 27° S early + KE north + LC 30° S (spawning season)	1.322	0.009	0.52225	4
	EKE south + LC 30° S (spawning season) + Xshore 29° S (spawning season)	1.446	0.009	0.58966	4
	CC 27° S early	1.735	0.008	0.1932	2
	EKE south + KE north + Xshore 31° S	1.755	0.008	0.53007	4
	KE north + LC 27° S (spawning season)	1.782	0.007	0.40766	3
	KE north + LC 30° S (spawning season) + Xshore 31° S (spawning season)	1.839	0.007	0.50423	4
	CC 27° S early + KE north + LC 27° S (spawning season)	1.895	0.007	0.49805	4
	KE north + KE South + LC 27° S (spawning season)	0	0.044	0.66194	4
Lancelin	KE south + LC 30° S (spawning season) + Xshore 27° S (spawning season)	0.977	0.027	0.54491	4
	EKE south + KE north + Xshore 31° S	1.26	0.023	0.5726	4
	KE north + KE South + Xshore 31° S	1.483	0.021	0.57312	4

Formatted Table

Formatted: Line spacing: single

Formatted: Line spacing: single

Formatted: Line spacing: single

Formatted: Line spacing: single

Formatted: Line spacing: single

Formatted: Line spacing: single

Formatted: Line spacing: single

Formatted: Line spacing: single

Formatted: Line spacing: single

Formatted: Line spacing: single

Formatted: Line spacing: single

Formatted: Line spacing: single

Formatted: Line spacing: single

Formatted: Line spacing: single

Formatted: Line spacing: single

Formatted: Line spacing: single

Formatted: Line spacing: single

Formatted: Line spacing: single

Formatted: Line spacing: single

Formatted: Line spacing: single

Formatted: Line spacing: single

Formatted: Line spacing: single

	<u>KE south + LC 27° S (spawning season)</u>	<u>1.711</u>	<u>0.019</u>	<u>0.68503</u>	<u>3</u>
	<u>KE north + KE south</u>	<u>1.911</u>	<u>0.017</u>	<u>0.53142</u>	<u>3</u>
	<u>EKE south + KE north + LC 27° S (spawning season)</u>	<u>1.953</u>	<u>0.017</u>	<u>0.60116</u>	<u>4</u>
	<u>KE north + KE South+ SST Winter</u>	<u>0</u>	<u>0.02</u>	<u>0.68482</u>	<u>4</u>
	<u>KE south + SST Winter</u>	<u>0.084</u>	<u>0.019</u>	<u>0.59854</u>	<u>3</u>
	<u>CC 27° S early + KE South + SST Winter</u>	<u>0.608</u>	<u>0.015</u>	<u>0.63389</u>	<u>4</u>
	<u>KE north</u>	<u>0.633</u>	<u>0.015</u>	<u>0.29904</u>	<u>2</u>
	<u>EKE South + KE north + SST Winter</u>	<u>0.91</u>	<u>0.013</u>	<u>0.6593</u>	<u>4</u>
	<u>EKE South + SST Winter</u>	<u>0.966</u>	<u>0.012</u>	<u>0.58518</u>	<u>3</u>
Alkimos	<u>KE South + SST Winter + Xshore 27° S (spawning season)</u>	<u>1.214</u>	<u>0.011</u>	<u>0.67061</u>	<u>4</u>
	<u>KE South + SST Summer + Xshore 31° S (spawning season)</u>	<u>1.392</u>	<u>0.01</u>	<u>0.57343</u>	<u>4</u>
	<u>CC 27° S early + EKE South + SST Winter</u>	<u>1.509</u>	<u>0.009</u>	<u>0.62109</u>	<u>4</u>
	<u>EKE North + KE South + SST Winter</u>	<u>1.535</u>	<u>0.009</u>	<u>0.66072</u>	<u>4</u>
	<u>KE north + KE South</u>	<u>1.838</u>	<u>0.008</u>	<u>0.48649</u>	<u>3</u>
	<u>EKE south + KE North</u>	<u>1.864</u>	<u>0.008</u>	<u>0.48183</u>	<u>3</u>
	<u>CC 27° S early + KE South + SST Summer</u>	<u>1.92</u>	<u>0.008</u>	<u>0.55349</u>	<u>4</u>
	<u>KE north+ SST Winter</u>	<u>1.967</u>	<u>0.008</u>	<u>0.36099</u>	<u>3</u>
	<u>Xshore 27° S + Xshore 31° S (spawning season)</u>	<u>0</u>	<u>0.01</u>	<u>0.63867</u>	<u>3</u>
	<u>LC 27° S winter</u>	<u>0.788</u>	<u>0.006</u>	<u>0.31409</u>	<u>2</u>
	<u>Xshore 27° S</u>	<u>1.115</u>	<u>0.005</u>	<u>0.34867</u>	<u>2</u>
	<u>CC 27° S early +LC 27° S winter</u>	<u>1.165</u>	<u>0.005</u>	<u>0.50841</u>	<u>3</u>
	<u>Xshore 29° S (spawning season)</u>	<u>1.166</u>	<u>0.005</u>	<u>0.26977</u>	<u>2</u>
	<u>Xshore 31° S (spawning season)</u>	<u>1.436</u>	<u>0.005</u>	<u>0.27396</u>	<u>2</u>
	<u>CC 30° S early (spawning season) + Xshore 27° S</u>	<u>1.579</u>	<u>0.004</u>	<u>0.47095</u>	<u>3</u>
	<u>LC 30° S (spawning season) + Xshore 31° S (spawning season)</u>	<u>1.62</u>	<u>0.004</u>	<u>0.37919</u>	<u>3</u>
Warnbro	<u>CC 27° S early</u>	<u>1.699</u>	<u>0.004</u>	<u>0.28026</u>	<u>2</u>
	<u>IBSS+ Xshore 31° S</u>	<u>1.701</u>	<u>0.004</u>	<u>0.50221</u>	<u>3</u>
	<u>CC 27° S early + Xshore 29° S</u>	<u>1.706</u>	<u>0.004</u>	<u>0.46989</u>	<u>3</u>
	<u>CC 27° S early + Xshore 31° S</u>	<u>1.719</u>	<u>0.004</u>	<u>0.44596</u>	<u>3</u>
	<u>LC 30° S (spawning season) + Xshore 27° S + Xshore 31° S (spawning season)</u>	<u>1.758</u>	<u>0.004</u>	<u>0.6657</u>	<u>4</u>
	<u>LC 27° S winter + Xshore 31° S</u>	<u>1.795</u>	<u>0.004</u>	<u>0.43706</u>	<u>3</u>
	<u>CC 27° S early + Xshore 29° S (spawning season)</u>	<u>1.805</u>	<u>0.004</u>	<u>0.4228</u>	<u>3</u>
	<u>Xshore 27° S + Xshore 29° S (spawning season)</u>	<u>1.986</u>	<u>0.004</u>	<u>0.50025</u>	<u>3</u>
	<u>Xshore 33° S (spawning season)</u>	<u>0</u>	<u>0.008</u>	<u>0.33639</u>	<u>2</u>
	<u>LC 27° S</u>	<u>0.008</u>	<u>0.008</u>	<u>0.39289</u>	<u>2</u>
	<u>Xshore 31° S (spawning season)</u>	<u>0.408</u>	<u>0.006</u>	<u>0.31403</u>	<u>2</u>
	<u>CC 30° S late (spawning season)</u>	<u>0.484</u>	<u>0.006</u>	<u>0.27898</u>	<u>2</u>
Cape Mentelle	<u>SST summer</u>	<u>0.484</u>	<u>0.006</u>	<u>0.34543</u>	<u>2</u>
	<u>CC 27° S early (spawning season)</u>	<u>0.676</u>	<u>0.006</u>	<u>0.20266</u>	<u>2</u>
	<u>LC 30° S (spawning season)</u>	<u>0.8</u>	<u>0.005</u>	<u>0.20202</u>	<u>2</u>
	<u>CC 34° S early (spawning season)</u>	<u>0.945</u>	<u>0.005</u>	<u>0.16214</u>	<u>2</u>
	<u>CC 34° S late (spawning season)</u>	<u>1.008</u>	<u>0.005</u>	<u>0.20141</u>	<u>2</u>

Formatted: Line spacing: single

Formatted: Line spacing: single

Formatted: Line spacing: single

Formatted: Line spacing: single

Formatted: Line spacing: single

Formatted: Line spacing: single

Formatted: Line spacing: single

Formatted: Line spacing: single

Formatted: Line spacing: single

Formatted: Line spacing: single

Formatted: Line spacing: single

Formatted: Line spacing: single

Formatted: Line spacing: single

Formatted: Line spacing: single

Formatted: Line spacing: single

Formatted: Line spacing: single

Formatted: Line spacing: single

Formatted: Line spacing: single

Bottom temperature	1.222	0.004	0.14284	2
CC 27° S late (spawning season)	1.262	0.004	0.16047	2
CC 27° S early	1.27	0.004	0.15818	2
EKE north	1.37	0.004	0.13383	2
Top 100m temp	1.446	0.004	0.12044	2
LC 34° S (spawning season)	1.528	0.004	0.10325	2
Xshore 33° S	1.533	0.004	0.09786	2
SST Winter	1.545	0.004	0.10168	2
IBSS	1.583	0.004	0.09485	2
CC 34° S early	1.702	0.003	0.05667	2
Xshore 31° S	1.806	0.003	0.04445	2
KE south	1.808	0.003	0.05125	2
Xshore 27° S (spawning season)	1.858	0.003	0.03529	2
EKE south	1.879	0.003	0.03523	2
Xshore 29° S (spawning season)	1.933	0.003	0.02133	2
Xshore 27° S	1.979	0.003	0.01187	2
KE north	1.979	0.003	0.01289	2

805 **Table A3. Top generalised additive models (GAMs) for predicting the late puerulus settlement at the eight sites from full subset analyses. Difference between lowest reported corrected Akaike Information Criterion (ΔAIC_c), AIC_c weight (ωAIC_c), variance explained (R^2) and effective degrees of freedom (EDF) are reported for model comparison. Model selection was based on the most parsimonious model (fewest variables) within two units of the lowest AIC_c , and models are ordered by parsimony.**

Site	Model	ΔAIC_c	ωAIC_c	R^2	EDF
Abrolhos	KE North	0	0.009	0.21872	2
	LC 27° S summer	0.456	0.007	0.1768	2
	KE North + LC 30° S winter	1.711	0.004	0.28972	3
	CC 30° S late (spawning season) + LC 27° S summer	1.904	0.003	0.30444	3
Port Gregory	IBSS + LC 30° S summer + Xshore 31° S	0	0.103	0.70071	4
	IBSS + LC 30° S (spawning season) + LC 30° S summer	1.151	0.058	0.57984	4
	IBSS + LC 30° S summer	1.639	0.046	0.62492	3
Dongara	IBSS + LC 30° S (spawning season)	0	0.021	0.45068	3
	IBSS	0.808	0.014	0.4202	2
	IBSS + KE North	1.984	0.008	0.48773	3
Jurien Bay	IBSS + LC 30° S (spawning season)	0	0.056	0.51808	3
	EKE north + IBSS + LC 30° S (spawning season)	1.301	0.029	0.58445	4
	CC 27° S early + IBSS + LC 30° S (spawning season)	1.702	0.024	0.55792	4
Lancelin	KE south	0	0.013	0.55565	2
	EKE south	0.599	0.01	0.51543	2
	Top 100m Temp	1.922	0.005	0.31946	2
	KE south+ Xshore 27° S (spawning season)	1.953	0.005	0.55691	3
Alkimos	EKE south + IBSS	1.96	0.005	0.47425	3
	KE south + LC 27° S winter	0	0.021	0.53502	3
	EKE south + LC 27° S winter	0.01	0.02	0.50903	3

Formatted: Font: 9 pt, Bold

Formatted: Font: 9 pt

Formatted: Font: 9 pt, Bold

Formatted: Font: 9 pt, Bold, Font color: Auto

Formatted: Font: 9 pt, Bold

	<u>CC 30° S late + EKE south + LC 27°S winter</u>	<u>1.852</u>	<u>0.008</u>	<u>0.60733</u>	<u>4</u>
	<u>CC 34° S early + LC 27° S winter</u>	<u>0</u>	<u>0.019</u>	<u>0.47117</u>	<u>3</u>
	<u>CC 34° S early + Xshore 27° S (spawning season)</u>	<u>1.153</u>	<u>0.01</u>	<u>0.39126</u>	<u>3</u>
<u>Warnbro</u>	<u>CC 34° S early + LC 27° S winter + LC 34° S summer</u>	<u>1.612</u>	<u>0.008</u>	<u>0.44042</u>	<u>4</u>
	<u>LC 27° S winter</u>	<u>1.705</u>	<u>0.008</u>	<u>0.42669</u>	<u>2</u>
	<u>CC 34° S early + IBSS</u>	<u>1.877</u>	<u>0.007</u>	<u>0.41882</u>	<u>3</u>
	<u>CC 30° S late (spawning season) + LC 27°S winter</u>	<u>1.973</u>	<u>0.007</u>	<u>0.61929</u>	<u>3</u>
<u>Cape</u>					
<u>Mentelle</u>	<u>Xshore 33° S (spawning season)</u>	<u>0</u>	<u>0.014</u>	<u>0.48806</u>	<u>2</u>

Formatted: Caption

Data Availability

The dataset for this research and relevant contacts can be found through the Department of Primary Industries and Regional Development website. <http://www.fish.wa.gov.au/Species/Rock-Lobster/Lobster-Management/Pages/Puerulus-Settlement-Index.aspx>

815 The ozROMS numerical model outputs are available at this THREDDS server <http://130.95.29.56:8080/thredds/catalog.html>

Author contribution

JK completed the analysis of the data and conclusions under the guidance of CH, TL, and SdL. JK wrote the manuscript and produced the figures with the help and inputs from all co-authors. TL developed the code for the multiple regression analysis (Fisher et al. 2016). All authors contributed to the article and approved the submitted version.

820 Competing interests

The authors declare that they have no conflict of interest

Acknowledgements

We would like to acknowledge the Department for Primary Industries and Regional Development (Fisheries) for the use of raw puerulus collector data. Thank you to Rebecca Fisher for her assistance with the multiple regression analysis toolbox.

825 Thank you to Sarath Wijeratne for ozROMS data processing assistance.

References

- Akaike, H.: Information theory and an extension of the maximum likelihood principle, *Second Int. Symp. Inf. Theory*, 267–281, 1973.
- 830 Andrews, J. C.: Eddy structure and the West Australian current, *Deep. Res.*, 24, 1133–1148, [https://doi.org/10.1016/0146-6291\(77\)90517-3](https://doi.org/10.1016/0146-6291(77)90517-3), 1977.
- Batteen, M. L., Kennedy, R. A., and Miller, H. A.: A process-oriented numerical study of currents, eddies and meanders in the Leeuwin Current System, *Deep. Res. Part II Top. Stud. Oceanogr.*, 54, 859–883, <https://doi.org/10.1016/j.dsr2.2006.09.006>,
- 835 2007.
- Benthuisen, J., Feng, M., and Zhong, L.: Spatial patterns of warming off Western Australia during the 2011 Ningaloo Niño: Quantifying impacts of remote and local forcing, *Cont. Shelf Res.*, 91, 232–246, <https://doi.org/10.1016/j.csr.2014.09.014>, 2014.
- Berthot, A., Pattiaratchi, C., Feng, M., Meyers, G., and Li, Y.: Understanding the natural variability of currents along the Western Australian coastline, The SRFME initiative and the SRFME collaborative linkages program, 2007.
- 840 Boening, C., Willis, J. K., Landerer, F. W., Nerem, R. S., and Fasullo, J.: The 2011 La Niña : So strong , the oceans fell, *Geophys. Res. Lett.*, 39, 1–5, <https://doi.org/10.1029/2012GL053055>, 2012.
- Bureau of Meteorology: Fremantle Mean Sea Level, 2021a.
- Bureau of Meteorology: Southern Oscillation Index, 2021b.
- 845 Burnham, K. and Anderson, D.: *Model Selection and Multimodel Inference*, Springer New York, 2002.
- Caballero, A., Pascual, A., Gerald, D., and Infantes, M.: Sea Level and Eddy Kinetic Energy variability in the Bay of Biscay inferred from satellite altimeter data, *J. Mar. Syst.*, 72, 116–134, <https://doi.org/10.1016/j.jmarsys.2007.03.011>, 2008.
- Caputi, N.: Impact of the Leeuwin Current on the spatial distribution of the puerulus settlement of the western rock lobster (*Panulirus cygnus*) and implications for the fishery of Western Australia, *Fish. Oceanogr.*, 17, 147–152, <https://doi.org/10.1111/j.1365-2419.2008.00471.x>, 2008.
- 850 Caputi, N. and Brown, R.: The effect of environment on puerulus settlement of the western rock lobster (*Panulirus cygnus*) in Western Australia, *Fish. Oceanogr.*, 2, 1–10, <https://doi.org/10.1111/j.1365-2419.1993.tb00007.x>, 1993.
- Caputi, N., Chubb, C., and Brown, R.: Relationships between Spawning Stock, Environment, Recruitment and Fishing Effort for the Western Rock Lobster, *Panulirus Cygnus*, Fishery in Western Australia, 68, 213–226, <https://doi.org/10.1163/156854095X00115>, 1995.
- 855 Caputi, N., Chubb, C., and Pearce, A.: Environmental effects on recruitment of the western rock lobster, *Panulirus cygnus*, *Mar. Freshw. Res.*, 52, 1167–1174, <https://doi.org/10.1071/MF01180>, 2001.
- Caputi, N., Melville-Smith, R., de Lestang, S., Pearce, A., and Feng, M.: The effect of climate change on the western rock lobster (*Panulirus cygnus*) fishery of Western Australia, *Can. J. Fish. Aquat. Sci.*, 67, 85–96, <https://doi.org/10.1139/F09-167>,
- 860 2010.

- Caputi, N., Feng, M., de Lestang, S., Denham, A., Penn, J., Slawinski, D., Pearce, A., Weller, E., and How, J.: Identifying factors affecting the low western rock lobster puerulus settlement in recent years, <https://doi.org/na>, 2014.
- Caputi, N., Chandrapavan, A., Kangas, M., de Lestang, S., Hart, A., Johnston, D., and Penn, J.: Stock-recruitment-environment relationships of invertebrate resources in Western Australia and their link to pro-active management harvest strategies, *Mar. Policy*, 133, 1–16, <https://doi.org/10.1016/j.marpol.2021.104728>, 2021.
- 865 Cetina-Heredia, P., Roughan, M., van Sebille, E., Feng, M., and Coleman, M.: Strengthened currents override the effect of warming on lobster larval dispersal and survival, *Glob. Chang. Biol.*, 21, 4377–4386, <https://doi.org/10.1111/gcb.13063>, 2015.
- Cetina-Heredia, P., Roughan, M., Liggins, G., Coleman, M., and Jeffs, A.: Mesoscale circulation determines broad spatio-temporal settlement patterns of lobster, *PLoS One*, 14, 1–20, <https://doi.org/10.1371/journal.pone.0211722>, 2019a.
- 870 Cetina-Heredia, P., Roughan, M., van Sebille, E., Keating, S., and Brassington, G.: Retention and Leakage of Water by Mesoscale Eddies in the East Australian Current System, *J. Geophys. Res. Ocean.*, 124, 2485–2500, <https://doi.org/10.1029/2018JC014482>, 2019b.
- Chittleborough, R.: Environmental factors affecting growth and survival of juvenile western rock lobsters *Panulirus longipes* (Milne-Edwards), *Mar. Freshw. Res.*, 26, 177–196, <https://doi.org/http://dx.doi.org/10.1071/MF9750177>, 1975.
- 875 Chittleborough, R.: Growth of Juvenile *Panulirus Longipes* Cygnus George on Coastal Reefs Compared with those Reared Under Optimal Environmental Conditions, *Mar. Freshw. Res.*, 27, 279–295, <https://doi.org/10.1071/MF9760279>, 1976.
- Chubb, C.: No Measurement of spawning stock levels for the western rock lobster *Panulirus cygnus*, *Rev. Investig. Mar.*, 12, 223–233, 1991.
- Clarke, A. and Li, J.: El Niño/La Niña shelf edge flow and Australian western rock lobsters, *Geophys. Res. Lett.*, 31, <https://doi.org/10.1029/2003GL018900>, 2004.
- 880 Cosoli, S., Pattiaratchi, C., and Hetzel, Y.: High-frequency radar observations of surface circulation features along the south-western australian coast, *J. Mar. Sci. Eng.*, 8, <https://doi.org/10.3390/jmse8020097>, 2020.
- Cresswell, G., Boland, F., Peterson, J., and Wells, G.: Continental shelf currents near the Abrolhos Islands, Western Australia, *Mar. Freshw. Res.*, 40, 113–128, <https://doi.org/10.1071/MF9890113>, 1989.
- 885 DeYoung, B., Harris, R., Alheit, J., Beaugrand, G., Mantua, N., and Shannon, L.: Detecting regime shifts in the ocean: Data considerations, *Prog. Oceanogr.*, 60, 143–164, <https://doi.org/10.1016/j.pocean.2004.02.017>, 2004.
- Ehrhardt, N. and Fitchett, M.: Dependence of recruitment on parent stock of the spiny lobster, *Panulirus argus*, in Florida, *Fish. Oceanogr.*, 19, 434–447, <https://doi.org/10.1111/j.1365-2419.2010.00555.x>, 2010.
- Fang, F. and Morrow, R.: Evolution, movement and decay of warm-core Leeuwin Current eddies, *Deep. Res. Part II Top. Stud. Oceanogr.*, 50, 2245–2261, [https://doi.org/10.1016/S0967-0645\(03\)00055-9](https://doi.org/10.1016/S0967-0645(03)00055-9), 2003.
- 890 Feng, M., Meyers, G., Pearce, A., and Wijffels, S.: Annual and interannual variations of the Leeuwin Current at 32 ° S, *J. Geophys. Res.*, 108, 19–39, <https://doi.org/10.1029/2002JC001763>, 2003.
- Feng, M., Wijffels, S., Godfrey, S., and Meyers, G.: Do eddies play a role in the momentum balance of the Leeuwin Current?, *J. Phys. Oceanogr.*, 35, 964–975, <https://doi.org/10.1175/JPO2730.1>, 2005.

- 895 Feng, M., Slawinski, D., Beckley, L., and Keesing, J.: Retention and dispersal of shelf waters influenced by interactions of ocean boundary current and coastal geography, *Mar. Freshw. Res.*, 61, 1259–1267, <https://doi.org/10.1071/MF09275>, 2010.
- Feng, M., Caputi, N., Penn, J., Slawinski, D., de Lestang, S., Weller, E., and Pearce, A.: Ocean circulation, Stokes drift, and connectivity of western rock lobster (*Panulirus cygnus*) population, *Can. J. Fish. Aquat. Sci.*, 68, 1182–1196, <https://doi.org/10.1139/f2011-065>, 2011.
- 900 Fisher, R., Wilson, S., Sin, T., Lee, A., and Langlois, T.: A simple function for full-subsets multiple regression in ecology with R, *Ecol. Evol.*, 8, 6104–6113, <https://doi.org/10.1002/ece3.4134>, 2018.
- Gersbach, G., Pattiaratchi, C., Ivey, G., and Cresswell, G.: Upwelling on the south-west coast of Australia - Source of the Capes Current, *Cont. Shelf Res.*, 19, 363–400, [https://doi.org/10.1016/S0278-4343\(98\)00088-0](https://doi.org/10.1016/S0278-4343(98)00088-0), 1999.
- Graham, M. H.: Statistical Confronting Multicollinearity in Ecological, *Source Ecol. Ecol.*, 84, 2809–2815, <https://doi.org/10.1890/02-3114>, 2009.
- 905 Griffin, D., Wilkin, J., Chubb, C., Pearce, A., and Caputi, N.: Ocean currents and the larval phase of Australian western rock lobster, *Panulirus cygnus*, *Mar. Freshw. Res.*, 52, 1187–1199, <https://doi.org/10.1071/MF01181>, 2001.
- Guan, L., Chen, Y., Wilson, J., Waring, T., Kerr, L., and Shan, X.: The influence of spatially variable and connected recruitment on complex stock dynamics and its ecological and management implications, *Can. J. Fish. Aquat. Sci.*, 76, 937–949, <https://doi.org/10.1139/cjfas-2018-0151>, 2019.
- 910 Hamon, B. : Geostrophic currents in the southeastern Indian Ocean, *Aust. J. Mar. Freshw. Res.*, 16, 255–271, 1965.
- Hood, R., Beckley, L., and Wiggert, J.: Biogeochemical and ecological impacts of boundary currents in the Indian Ocean, *Prog. Oceanogr.*, 156, 290–325, <https://doi.org/10.1016/j.pocean.2017.04.011>, 2017.
- Huang, Z. and Feng, M.: Remotely sensed spatial and temporal variability of the Leeuwin Current using MODIS data, *Remote Sens. Environ.*, 166, 214–232, <https://doi.org/10.1016/j.rse.2015.05.028>, 2015.
- 915 Hurvich, C. and Tsai, C.: Biometrika Trust Regression and Time Series Model Selection in Small Samples, *Biometrika*, 76, 297–307, 1989.
- Kolbusz, J., de Lestang, S., Langlois, T., and Pattiaratchi, C.: Changes in *Panulirus cygnus* settlement along Western Australia using a long time series, *Front. Mar. Sci.*, 8, <https://doi.org/10.3389/fmars.2021.628912>, 2021.
- 920 Koslow, J., Pesant, S., Feng, M., Pearce, A., Fearn, P., Moore, T., Matear, R., and Waite, A.: The effect of the Leeuwin Current on phytoplankton biomass and production off Southwestern Australia, *J. Geophys. Res. Ocean.*, 113, 1–19, <https://doi.org/10.1029/2007JC004102>, 2008.
- Lenanton, R., Joll, L., Penn, J., and Jones, K.: The influence of the Leeuwin Current on coastal fisheries of Western Australia, *J. R. Soc. West. Aust.*, 74, 101–114, 1991.
- 925 de Lestang, S., Caputi, N., How, J., Melville-Smith, R., Thomson, A., and Stephenson, P.: Stock assessment for the west coast rock lobster fishery, *Fisheries Research Report No. 217*, 1–200 pp., 2012.
- de Lestang, S., Caputi, N., Feng, M., Denham, A., Penn, J., Slawinski, D., Pearce, A., and How, J.: What caused seven consecutive years of low puerulus settlement in the western rock lobster fishery of Western Australia?, *ICES J. Mar. Sci.*, 72,

- 49–58, <https://doi.org/10.1093/icesjms/fst048>, 2015.
- 930 de Lestang, S., Caputi, N., and How, J.: Resource Assessment Report: Western Rock Lobster Resource of Western Australia, Western Australian Marine Stewardship Council Report Series No. 9, Western Australian Marine Stewardship Council Report Series, 1–139 pp., 2016.
- de Lestang, S., Rossbach, M., and Blay, N.: West Coast Rock Lobster Resource Status Report 2017. In: Status Reports of the Fisheries and Aquatic Resources of Western Australia 2016/17: The State of the Fisheries, 2018.
- 935 Luo, H., Bracco, A., and Di Lorenzo, E.: The interannual variability of the surface eddy kinetic energy in the Labrador Sea, *Prog. Oceanogr.*, 91, 295–311, <https://doi.org/10.1016/j.pocean.2011.01.006>, 2011.
- MATLAB: Matlab R2019b, Natick, Massachusetts: The MathWorks Inc., 2019.
- Medel, C., Parada, C., Morales, C., Pizarro, O., Ernst, B., and Conejero, C.: How biophysical interactions associated with sub- and mesoscale structures and migration behavior affect planktonic larvae of the spiny lobster in the Juan Fernández Ridge: A modeling approach, *Prog. Oceanogr.*, 162, 98–119, <https://doi.org/10.1016/j.pocean.2018.02.017>, 2018.
- 940 Menezes, V., Phillips, H., Schiller, A., Bindoff, N., Domingues, C., and Vianna, M.: South Indian Countercurrent and associated fronts, *J. Geophysical Res. Ocean.*, 119, 6763–6791, <https://doi.org/doi:10.1002/2014JC010076>, 2014.
- Meuleners, M., Ivey, G., and Pattiaratchi, C.: A numerical study of the eddying characteristics of the Leeuwin Current System, *Deep. Res. Part I Oceanogr. Res. Pap.*, 55, 261–276, <https://doi.org/10.1016/j.dsr.2007.12.004>, 2008.
- 945 Nieto, K., McClatchie, S., Weber, E., and Lennert-Cody, C.: Effect of mesoscale eddies and streamers on sardine spawning habitat and recruitment success off Southern and central California, *J. Geophys. Res. Ocean.*, 119, 6330–6339, <https://doi.org/10.1002/2014JC010251>, 2014.
- O’Rorke, R., Jeffs, A., Wang, M., Waite, A., Beckley, L., and Lavery, S.: Spinning in different directions: western rock lobster larval condition varies with eddy polarity, but does their diet?, *J. Plankton Res.*, 37, 542–553, <https://doi.org/10.1093/PLANKT/FBV026>, 2015.
- 950 Pattiaratchi, C. and Buchan, S.: Implications of long-term climate change for the Leeuwin Current, *J. R. Soc. West. Aust.*, 74, 133–140, 1991.
- Pattiaratchi, C. and Hetzel, Y.: Sea surface temperature variability: State and trends of Australia’s oceans report, Hobart, 1.2.1–1.2.4 pp., 2020.
- 955 Pattiaratchi, C. and Siji, P.: Variability in ocean currents around Australia: State and trends of Australia’s oceans report, Hobart, 1.4.1–1.4.6 pp., 2020.
- Pattiaratchi, C. and Woo, M.: The mean state of the Leeuwin Current system between North West Cape and Cape Leeuwin, *J. R. Soc. West. Aust.*, 92, 221–241, 2009.
- Pattiaratchi, C., Hegge, B., Gould, J., and Eliot, I.: Impact of sea-breeze activity on nearshore and foreshore processes in southwestern Australia, *Cont. Shelf Res.*, 17, 1539–1560, [https://doi.org/10.1016/S0278-4343\(97\)00016-2](https://doi.org/10.1016/S0278-4343(97)00016-2), 1997.
- 960 Pawlowicz, R.: M_Map: A mapping package for MATLAB, Version 1.4m, 2020.
- Pearce, A. and Griffiths, R.: The mesoscale structure of the Leeuwin Current: a comparison of laboratory models and satellite

- imagery, *J. Geophys. Res.*, 96, <https://doi.org/10.1029/91jc01712>, 1991.
- Pearce, A. and Pattiaratchi, C.: The Capes Current: A summer countercurrent flowing past Cape Leeuwin and Cape Naturaliste, *Western Australia, Cont. Shelf Res.*, 19, 401–420, [https://doi.org/10.1016/S0278-4343\(98\)00089-2](https://doi.org/10.1016/S0278-4343(98)00089-2), 1999.
- 965 Pearce, A. and Phillips, B.: Enso events, the leeuw current, and larval recruitment of the western rock lobster, *ICES J. Mar. Sci.*, 45, 13–21, <https://doi.org/10.1093/icesjms/45.1.13>, 1988.
- Phillips, B.: The circulation of the southeastern Indian Ocean and the planktonic life of the western rock lobster, *Oceanogr. Mar. Biol. Annu. Rev.*, 19, 11–39, <https://doi.org/10.1071/MF9810417>, 1981.
- 970 Phillips, B.: Prediction of Commercial Catches of the Western Rock Lobster (*Panulirus cygnus*), *Can. J. Fish. Aquat. Sci.*, 43, 2126–2130, 1986.
- Rennie, S., Pattiaratchi, C., and Mccauley, R.: Eddy formation through the interaction between the Leeuwin Current, Leeuwin Undercurrent and topography, *Deep. Res. Part I Oceanogr. Res. Pap.*, 54, 818–836, <https://doi.org/10.1016/j.dsr2.2007.02.005>, 2007.
- 975 Sävström, C., Beckley, L., Saunders, M., Thompson, P., and Waite, A.: The zooplankton prey field for rock lobster phyllosoma larvae in relation to oceanographic features of the south-eastern Indian Ocean, *J. Plankton Res.*, 36, 1003–1016, <https://doi.org/10.1093/plankt/fbu019>, 2014.
- Schiller, A., Oke, P., Brassington, G., Entel, M., Fiedler, R., Griffin, D., and Mansbridge, J.: Eddy-resolving ocean circulation in the Asian-Australian region inferred from an ocean reanalysis effort, *Prog. Oceanogr.*, 76, 334–365, <https://doi.org/10.1016/j.pocean.2008.01.003>, 2008.
- 980 Smith, R., Huyer, A., Godfrey, S., and Church, J.: The Leeuwin Current off Western Australia, 1986-1987, *J. Phys. Oceanogr.*, 21, 323–345, [https://doi.org/10.1175/1520-0485\(1991\)021<0323:TLCOWA>2.0.CO;2](https://doi.org/10.1175/1520-0485(1991)021<0323:TLCOWA>2.0.CO;2), 1991.
- Wang, M., O'Rorke, R., Waite, A., Beckley, L., Thompson, P., and Jeffs, A.: Condition of larvae of western rock lobster (*Panulirus cygnus*) in cyclonic and anticyclonic eddies of the Leeuwin Current off Western Australia, *Mar. Freshw. Res.*, 66, 1158–1167, <https://doi.org/10.1071/MF14121>, 2015.
- 985 Wernberg, T., Smale, D., Tuya, F., Thomsen, M., Langlois, T., de Bettignies, T., Bennett, S., and Rousseaux, C.: An extreme climatic event alters marine ecosystem structure in a global biodiversity hotspot, *Nat. Clim. Chang.*, 3, 78–82, <https://doi.org/10.1038/nclimate1627>, 2012.
- Wickham, H., Francois, H., and Muller, K.: dplyr: A Grammar of Data Manipulation. R package version 0.7.6, 2018.
- 990 Wijeratne, S., Pattiaratchi, C., and Proctor, R.: Estimates of surface and subsurface boundary current transport around Australia, *J. Geophys. Res. Ocean.*, 123, 3444–3466, <https://doi.org/10.1029/2017JC013221>, 2018.
- Wijffels, S., Beggs, H., Griffin, C., Middleton, J., Cahill, M., King, E., Jones, E., Feng, M., Benthuisen, J., Steinberg, C., and Sutton, P.: A fine spatial-scale sea surface temperature atlas of the Australian regional seas (SSTAARS): Seasonal variability and trends around Australasia and New Zealand revisited, *J. Mar. Syst.*, 187, 156–196, <https://doi.org/10.1016/j.jmarsys.2018.07.005>, 2018.
- 995 Woo, M. and Pattiaratchi, C.: Hydrography and water masses off the western Australian coast, *Deep. Res. Part I Oceanogr.*

Res. Pap., 55, 1090–1104, <https://doi.org/10.1016/j.dsr.2008.05.005>, 2008.

Wood, S. N.: Generalized Additive Models: An Introduction with R, Second Edition, CRC Press, 2017.

1000 Yeung, C., Jones, D., Criales, M., Jackson, T., and Richards, W.: Marine freshwater influence of coastal eddies and counter-currents on the influx of spiny lobster, *Mar. Freshw. Res.*, 52, 1217–1232, 2001.

1005